Faculdade de Engenharia da Universidade do Porto

Rehabilitation of the ACL using Synthetic Reinforcements: A Biomechanical Study

João Pedro Lopes Moreira

junho de 2020

Faculdade de Engenharia da Universidade do Porto

Rehabilitation of the ACL using Synthetic Reinforcements: A Biomechanical Study

João Pedro Lopes Moreira

Dissertação realizada no âmbito do
Mestrado em Engenharia Biomédica

Orientador: Prof. Marco Parente – FEUP/INEGI
Coorientador: Doutora Nilza Ramião - INEGI

Junho 2020

Abstract

The knee joint is a complex structure with various components, each with their specific characteristics from their geometry, composition, biomechanics to their interactions with each other.

This joint, being responsible for providing both stability and motion to the knee, when it is injured the consequences can be very serious.

Unfortunately, this structure can be easily jeopardized when significant damage is done to its components. The ACL being one of the more commonly injured structures and, possibly, causing more devastating effects to the integrity of the joint.

Treatments currently used are mainly surgical, with arthroscopic anatomic grafting being a popular technique which consists in grafting organic or synthetic tissue to the damaged ACL area. There are three types of grafts in this technique, but the focus of this work will be on synthetic ligament grafts.

The objective of this work is to create a model of the Knee joint, introduce a synthetic graft reinforcement into its Anterior Cruciate Ligament and analyse the behaviour of the joint through the Finite Element method.

The simulations were performed with a posterior force, of 134N, applied to the Femur and the Tibia constrained on all degrees of freedom. The tests were performed on rotation angles of 0°, 15° and 30°.

The results showed that the Reinforcement, with the material properties given here, did not provide enough stability to the knee causing other components, namely both menisci, the Tibial and Femoral cartilage, to be under higher stress values than they would normally be in the same conditions.

The Finite Element method proved to be a great tool, capable of providing accurate simulations at a relative low cost and with time efficiency when compared to the ex-vivo/in-vivo methodologies. But like mentioned previously, the knee joint is a complex structure, making the creation of a perfectly accurate simulation a big challenge.

Resumo

A articulação do joelho é uma estrutura complexa que possui vários componentes, cada um com as suas características específicas, desde geometria, composição e biomecânica até às suas interações entre si.

Esta articulação, sendo responsável por fornecer estabilidade e movimento ao joelho, quando se encontra lesionada, as consequências podem ser muito graves.

Infelizmente, esta estrutura pode ser facilmente comprometida quando danos significativos são causados a um dos seus componentes. O Ligamento Cruzado Anterior é uma das estruturas que se danifica com maior facilidade, possivelmente causando efeitos devastadores à integridade da articulação.

Os tratamentos atualmente utilizados são principalmente cirúrgicos, sendo o enxerto anatômico artroscópico a técnica mais popular. Esta consiste em usar um enxerto de tecido orgânico ou sintético e colocá-lo na área do Ligamento Cruzado Anterior danificada. Existem três tipos de enxertos, mas o foco deste trabalho será o enxerto de ligamentos sintéticos.

O objetivo deste trabalho é criar um modelo da articulação do joelho, introduzir um reforço de enxerto sintético no seu Ligamento Cruzado Anterior e analisar o comportamento da articulação pelo método dos elementos finitos.

As simulações foram realizadas com uma força posterior, de 134N, aplicada no fêmur enquanto a tíbia se encontre restrita em todos os seus graus de liberdade. Os testes foram realizados em ângulos de rotação de 0°, 15° e 30°.

Os resultados obtidos mostraram que o Reforço, com as propriedades de material fornecidas aqui, não proporcionou estabilidade suficiente ao joelho fazendo com que outros componentes, como os meniscos, a cartilagem tibial e femoral, estivessem sob valores de stress mais elevados do que normalmente estariam nas mesmas condições.

O método dos elementos finitos provou ser uma ótima ferramenta, capaz de fornecer simulações precisas a um custo relativamente baixo e com eficiência de tempo quando comparado às metodologias ex vivo/in vivo. Mas, como mencionado anteriormente, a articulação do joelho é uma estrutura complexa, tornando a criação de uma simulação completamente precisa um grande desafio.

Agradecimentos

Terminando esta dissertação, gostaria de agradecer a todas as pessoas que ajudaram para a realização da mesma.

Começo por agradecer ao meu orientador, Doutor Marco Parente, pelo continuado acompanhamento e toda a disponibilidade mostrada, toda a ajuda, esforço e paciência dados para fornecer as melhores condições possíveis para a realização do presente trabalho.

À Doutora Nilza Ramião, que desempenhou o papel de coorientadora, agradeço a disponibilidade e apoio no esclarecimento de dúvidas e da ajuda na obtenção do variado material teórico.

Aos vários amigos e colegas que fiz ao longo destes anos, que tornaram todo este percurso uma experiência consideravelmente mais memorável.

À minha família (meu pai, minha mãe, minha irmã e restantes familiares), que durante todo o meu percurso académico partilharam todos os meus bons e maus momentos e bons e maus resultados, sem o apoio deles nunca teria sido possível estar onde me encontro neste momento.

Index

Figure List

Table List

List of Acronyms and Symbols

List of Acronyms

ACL	Anterior Cruciate Ligament
AMB	Anteromedial Bundle
CAE	Complete Abaqus Environment
FE	Finite Element
FEA	Finite Element Analysis
FEM	Finite Element Method
LARS	Ligament Advanced Reinforcement System
LCL	Lateral Collateral Ligament
MCL	Medial Collateral Ligament
PCL	Posterior Cruciate Ligament
PLB	Posterolateral bundle
PET	Polyethilene Plyester

List of Symbols

S	Coordinate System-Referential
U	Offset field
A	Nodal dislocation
N	Interpolating Function or Shape Function
δ	Normal Stress
p’	Distributed outer action
C	Coefficient term of a polynomial
I	Exact value of an integral
J	Integral value calculated according to Gauss quadrature
P	Position of a Gauss Point or Sampling Point (Gauss Quadrature)
W	Weight associated with a Gauss point or sampling point
E	Young’s Modulus (or Elastic Modulus)
υ	Poisson’s Ratio
$\boldsymbol{\Psi}$	Strain Energy Density Function

κ	Dispersion Parameter
$\boldsymbol{F}$	Deformation Gradient
$I1$	First Strain Invariant
$I2$	Second Strain Invariant
$I3$	Third Strain Invariant
$\overline{I_1}$	Isochoric Component of the First Strain Invariant
$\overline{I_4}$	Isochoric Component of the Fourth Invariant
$\overline{I_6}$	Isochoric Component of the Sixth Invariant
$\boldsymbol{a}_{04,06}$	Unit vectors that define the preferred direction of one family of fibers in the reference conFiguretion
$\overline{C}$	Isochoric Right Cauchy-Green Deformation Tensor
$\boldsymbol{C}$	Right Cauchy-Green Deformation Tensor
$C10$	Neo-Hookean Parameter
$k1$, $k2$	Parameters of the HGO Model Anisotropic Component
ε	Uniaxial Strain
λ	Stretch Ratio
ρ	Statistical distribution function

Chapter 1

Introduction

The knee is one of the most complex and largest articulations on the human body, being the point in which the femur, tibia and the patella converge. The knee joint has the role of bearing high loads and allow the necessary mobility for locomotion [1,2].

Besides its bony structure this joint is also constituted by articular cartilage, menisci and ligaments whose mechanical interactions will be explained further later on this report.

The ligaments provide stability to the joint, with the main ones being the four major ligaments supporting the knee. These include the Anterior Cruciate Ligament (ACL), the Posterior Cruciate ligament (PCL), the Medial Collateral ligament (MCL) and the Lateral Collateral ligament (LCL). The ACL, in conjunction with the PCL, is a crucial component of the knee which provides stability to the joint in everyday movement and loading activities, by preventing knee hyperextension and restraining tibial translation [3,4,5,6,7,8].

1.1 - Motivation

Unfortunately, ACL rupture is a very common ligament injury, its location making it prone to high load stress [7]. ACL rupture, besides inducing pain, severely compromises the joint's functionality by altering its kinematics, causing local instability, altering the rotation centre of the knee and the tibiofemoral contact area depending on its severity. A major problem resulting from these injuries is the high possibility of it causing secondary lesions on other parts of the joint like the menisci and articular cartilage [3,4,7,9].

A field in which ACL injury is very common and especially destructive is in sports, mainly those associated with extreme physical load on the athlete's legs. For example, sports which demand activities based on jump-landing tasks and side-step cutting activities such as soccer, basketball or tennis [3,7,9-12]. For these athletes ACL rupture is a possible career ending injury since it requires an expensive treatment and a long span of time until full recovery, with the possibility of complete recovery not happening and leaving them with a severe diminished knee mobility and the chance of developing osteoarthritis. [3,6,7,10]

Current methods to restore a completely torn ACL are mainly surgical, based on the replacement of the missing tissue through grafts. These methods use a patellar tendon or ham-

strings tendon graft; however, studies have shown that these techniques substantially alter the biomechanics of the knee compromising the normal interaction between the joint and the cartilage below, exponentially increasing the risk of Osteoarthritis [4,11-13].

Therefore, research for new techniques and methodologies has been a focus, leading to the rise in popularity of synthetic reinforcement grafts, which will be mentioned in detail later.

There have been several studies performed on the biomechanics and kinematics of the knee joint, mainly focusing on the ACL and its role. These studies had aimed to better understand ACL injuries and their causes, in order to learn how to prevent them and to improve surgical procedures.

To achieve these aims, several methodologies have been used, such as: ex vivo techniques [14-17], clinical studies, in vivo evaluations [14,18-20] and computerized simulations.

The first two have many advantages, but also have major disadvantages and limitations such as the difficulties involved in reproducing natural, pathological and degenerative conditions, the complexity involved in reproducing and measuring strains and forces on the various joint components and the high cost associated with these methodologies [21-23].

These problems do not manifest as severally on computational simulations, being the better alternative to study the knee joints biomechanically with comparably reduced cost and high efficiency, obviously depending on the robustness of the simulation hardware used [21,24-26].

The Finite Element analysis method (FEM) specifically is a very important tool, for computational simulation, capable of providing accurate results with certain reliability [12,14]. However, the knee joint is an extremely complex structure, and its computerized simulation is still not perfectly applied today, the complexity of this joint stems from its component's material properties and interactions with each other [6,14,22,25-26].

However, when a balance between the model's complexity and computational efficiency is achieved, the FEM analysis still proves that it is the more suitable tool in providing clinically useful biomechanical results.

1.2 - Literature Review

Several research works have been performed in the past years with the objective of improving our knowledge and comprehension on the knee joint and its components, many different models have been developed in order to simulate joint biomechanics, kinematics and the role of its various components. These served has a starting point for this study and will be presented below.

One of the first models developed with this intent was the four-bar linkage model, in 1917 Lehrbuch der Muskel and Gelenkmechanik [27] were one of the firsts to publish works with this model, see figure 1 below.

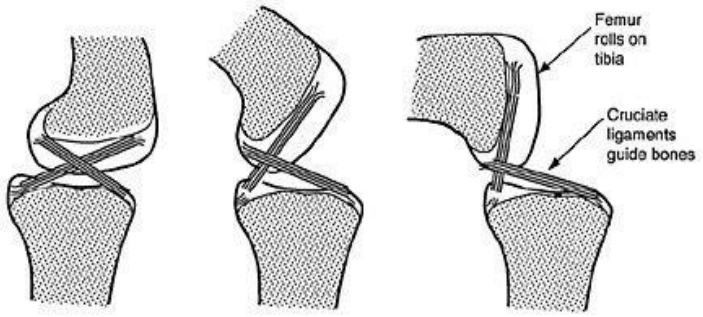

Figure 1.1 – Four bar linkage model, adapted from [28]

The model, as seen in figure 1, defined the cruciate ligaments as rigid bars in the sagittal plane and the point in which these bars crossed each other was the centre of rotation of the joint, it had a closed loop mechanism that allowed for a combination of rotation and translation movements in the sagittal plane without the need to have artificial ligaments to keep the rigidity of the system [27,29,30,31]. The main advantages of this model were its capability to simulate the shape of the articular surfaces, the relative movement of the rotational axis and the behaviour of the cruciate ligaments during anterior/posterior drawer motion; the disadvantages/limitations were its incapability of simulating knee laxity, the behaviour of the other ligaments and motion in the transversal planes [30].

Later a variation of this model was introduced called the crossed four-bar linkage model, which had improved the motion of the model, in the sagittal plane, closer to that of a human knee but with limited ranges of motion [32,33]. Many iterations and improvements to these models were made since, but from here on the focus will be on FE models.

Until today there have been a number of attempts at creating knee joint FE models; these vary from each other depending on the parameters in which they were developed, like geometry definition and what loads were intended to be simulated, application, material properties, etc.

The application for the model may be more generalized or specific depending on the complexity of the components or lack thereof, even simplifications made in these models differentiate them, some FE models focus solely on the tibio-femoral part [22,23,26,31,34-36] or simply do not include some components like the menisci, specific ligaments or articular cartilage [22,23,34,36] in order to simplify their analysis.

The material properties used for the various components is another complex topic with some still not having a globally agreed definition, the ligaments specifically are a big challenge since there isn't an infallible material model capable of perfectly simulating their non-linear behaviour. The material properties commonly used to define knee ligaments in current studies are: anisotropic hyper-elastic [14], isotropic [22,23] and transversely isotropic [12,21,36,37]. A study performed by Wan et al. [31] compared the use of these material definitions. It is concluded that none of the three models can describe all the different behaviours that the ligaments may have when under longitudinal or transverse tension and finite simple shear, the results also showed that the models tested had similar force results, but the kinematic response of the joint and stress distribution varied between them.

As for the type of analysis, knee joint FE analysis can be performed as a static analysis [12,14], quasi-static analysis [1,14,22,23,26,34,34,35,38] or dynamic analysis [14,34,39-41]; depending on the type motion and what results are intended.

Focusing on FE modelling of the ligament components of the knee joint, simplifying the ligaments as one-dimensional truss-beams [1,40] or springs elements [26,39,38], is an option that makes the calculations related to their behaviour easier and help provide faster results regarding knee kinematics. But this simplification has its disadvantages since this type of model isn't capable of showing the stress distribution in the said ligament [22]. Therefore, in order to obtain more accurate results, it has been concluded that the knee FE model should have a three-dimensional representation of the ligaments [30].

Some models also apply an initial strain to the model [1,12,21,23,26,37,39,40], this is done in order to try and replicate the in vivo residual stresses that the ligaments are under in order to make the model as close to reality as possible.

Even though the creation of a FE knee joint model is a complex subject, as explained above, its development has been a topic of great interest for many reasons.

Ali Kiapour et al. [14] performed a study that used the FE model of the knee to investigate injury mechanisms. The model used was validated against tibio-femoral kinematics, ligaments strain/force and articular cartilage pressure from static, quasi-static and dynamic experiments. The results showed that the model was capable of predicting the kinematics of the joint and stress/strain fields on the biological tissue with all the model's predictions being within 95% confidence intervals average experimental data.

Georges L. et al. [42] used the FE analysis method in order to research the human ACL when subjected to passive anterior tibial loads. In this article a 3D continuum FE model of the ACL was developed and used to simulate clinical knee procedures namely the Lachman and drawer tests. The objective here was to evaluate the existence and severity of an ACL knee injury by analysing the model joint starting on a flexed position, at 30° for the Lachman test and 90° for the drawer test, followed by an anterior tibial displacement of 4mm. The results obtained showed that both tests have different effects on the ACL's behaviour, showing that at 30° of flexion stress mainly appears in the mid anterolateral portion of the ACL and as flexion increases the stress that the anteromedial part of the ACL becomes the most stressed.

G. Limbert et al. [12] studied a three-dimensional FE model of the human ACL from experimental measurements on cadaveric knee specimen which were subjected to kinematic tests, to perform simulations of passive knee flexion with and without pre-stressing the ACL and assess the stress distribution on the ligament. They verified that, when the ACL was pre-stressed, the stress distribution values were within the predicted results and resembled the values reported in literature; between the pre-stressed and stress-free ACL the results were similar, but at lower flexion angles, the pre-stressed ACL had higher values of stress distribution.

Hyung-Soon Park et al. [34] presented a FE analysis of the ACL impingement against the intercondylar notch during external rotation and abduction of the tibia for noncontact injuries. This research showed that impingement between the lateral wall of the intercondylar notch and the ACL may occur when the knee rotates externally 29.1° and abducted at 10° resulting in strong contact pressure and tensile stress on the ACL. With the results obtained, namely the impact force (at 36.9N) and contact area (at 19.7 mm^2), on par with their cadaver counterparts.

Peña et al. [37] developed a three-dimensional FE simulation of the human knee joint in order to study the effect of graft stiffness and tensioning in ACL reconstruction and joint biomechanics. The analysis was performed at tension values of 0, 20, 40 and 60 N, at flexion angles of 0°, 30° and 60° and with three different grafts, namely patellar tendon graft, gracilis graft and quadrupled semitendinosus graft. With the results obtained it was concluded that the best graft tested was the patella tendon graft exhibiting a pretension of 60N, but this pretension causes additional stress in the graft during movement which in turn may hinder the revascularization and remodelling during the healing process therefore a lower pretension at 40N was recommended.

Benjamin J. Ellis et al. [35] studied the effect of ACL deficiency on MCL insertion site and contact forces during anterior tibial and valgus loading using FE model. The results obtained showed that when in an ACL deficiency knee there is an increase in MCL insertion site and contact forces, this happens due to the subsequent increase in anterior tibial loading. But in contrast this increase does not happen in response to valgus loading. So, with these results, it was concluded that the ACL does not take part in valgus rotation restraint in the knee.

K.E. Moglo and A. Shirazi-Adl [26] tested the biomechanics of a passive knee joint during drawer load (100N posterior femoral force at flexion angles between 0° to 90°) in intact and ACL deficient knee joint using a non-linear three-dimensional FE model of a tibiofemoral knee joint with the bony structures, the articular cartilage, menisci and the four major ligaments. The data obtained indicated the ACL as the main structure that resists drawer load, within the ranges of flexion studied, and that its absence would increase the primary and coupled laxities of the joint.

1.3 – Objectives and Structure

The main goal of this study is to create a Model of the knee joint through the FE method that is capable of simulating the biomechanical behaviour of the joint with an ACL reinforced by a synthetic graft. The results obtained should provide a clinically relevant case for the reliability of said synthetic grafts in maintaining the overall stability of the knee joint through stress and force distribution data.

Ultimately it is desired that the model be capable of reproducing qualitative, and if possible, quantitative results comparable to the data found in literature providing a reliable starting point for future work related to the study.

This dissertation will be divided into seven chapters. The first chapter is for introductory purposes containing the motivation behind this study as well as some general concepts and its objectives, it also contains a literature review on the work already done on the fields that concern this study from the knee joint biomechanics to the FE methodologies.

Chapter two will contain an in-depth look into the aspects and theoretical concepts that this work is based on, starting on the human skeleton system its joints and going into the anatomical aspects of the various components of the knee and their biomechanics. The next chapter has an extensive overview on ACL injuries their causes, consequences and treatments, as well as an introduction into ACL synthetic graft reinforcements.

Chapter five details the FE methodology and some theory in order to comprehend it. In this chapter some detailed information on the final model and the files that compose it is also presented.

Chapter six contains the results obtained from the simulation tests performed, these include the stress and reaction force data for the whole model and the relevant ligaments, and the discussion of said results.

In chapter seven the conclusions of the study and the future work suggestions for further development of the model are presented.

At the end the references used throughout the development of this study are given as well as appendices that contain additional relevant information.

Chapter 2

Anatomy

The human body is an incredibly complex biological machine composed by a great number systems, in this chapter some of these systems will be explored in the context of this work.

2.1 - The Human Skeletal System

The human skeletal system, figure 2, is composed by the bones of the skeleton, the ligaments, cartilage and the connective tissue.

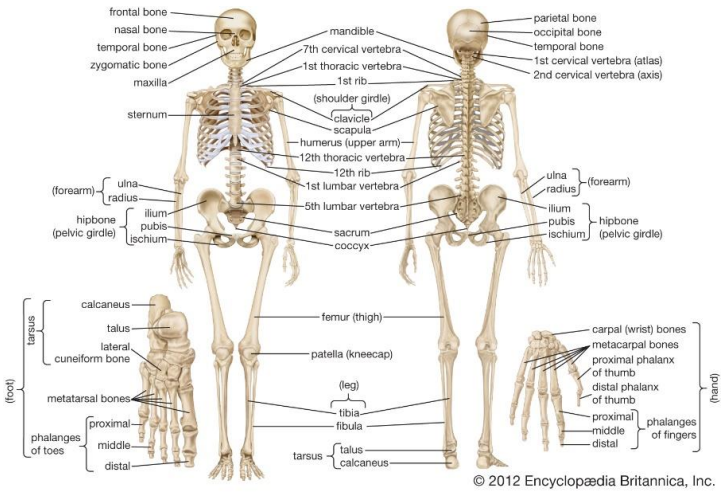

Figure 2.1 – Complete human skeletal system [43]

This system has various roles namely: [8]

- Provide support through its rigid bones, which also provide the body with the framework for its shape and structural support, and the cartilage that also serves to shape some parts of the human body like the nose and external ears; all of these are kept together through the ligaments and connective tissue.
- Enables locomotion through the skeletal muscles which are connected to the bones and, when contracted, make the bones act as levers that transmit the force that they

generate. Through the tendons and ligaments, the extent and direction of the force can be changed affecting the complexity of the movement.

- Storage, the bones possess a storage of essential minerals like calcium, magnesium and phosphorous. And the concentration of these minerals in the body drops below normal levels these minerals are released from the bones to the blood stream.
- Protection, bone being a rigid structure, is placed in the human body enveloping crucial body parts like the internal organs. The brain is protected by the skull, the lungs and heart are protected by the sternum and ribs, the spinal cord is protected by the vertebrae, the abdominal digestive and reproductive systems are protected by the pelvis.
- Blood cell production, possible through the red bone marrow located within most bones.

There are 206 bones in total on the human body, all of these are classified according to their shape: long bones, short bones, flat bones, irregular and sesamoid bones.

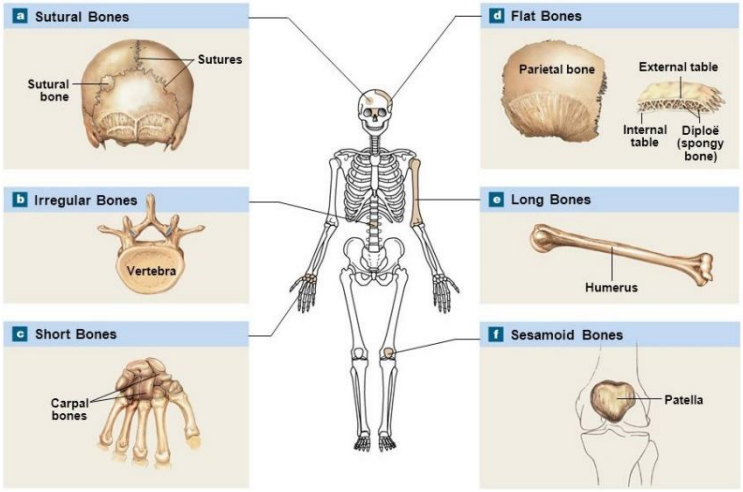

Figure 2.2 – Classification of the bones in the Human Body [45]

Long bones are bones whose length exceeds their width, these bones include the humerus, radios, ulna, femur, tibia, etc. Long bones usually possess a diaphysis composed of compact bone and a metaphysis composed of cancellous bone. Past the metaphysis, in the extremities of the bone, are located the epiphysis the line that separates these is called the epiphyseal line. The diaphysis on long bones is usually thicker towards the middle, this in mainly because that is where most of the strain is located [8].

Short bones, like the name entails, are short and compact bones. These bones are located on parts of the body in which a lot of movement is not required, i.e. the wrist and tarsal bones [8].

Flat bones are thin bones that are usually found in locations in which there is muscle attachment or protection of soft tissue needed, thanks to their surface that allows for it. These bones are mostly curved composed by cancellous bone and compact tissue. Examples of these are the ribs and scapula [8].

Irregular bones to put it simply, are bones that do not fit the criteria of the previous categories being peculiar and unique. Some of these bones include the vertebrae, ossicles of the ear, coccyx, etc.

The patella on the knee is a sesamoid bone, this type of bone is described as small and round located within tendons with the role of assisting in muscle function [8].

Now going back to the bone composition, the lamellar or mature osseous tissue can be classified into two types: cancellous or trabecular tissue and cortical or compact tissue. Even though these tissues have the same constituent elements they differ in their structural organization and functionality.

The spongy bone tissue is formed by thin trabeculae, these consisting of bony lamellae, parallel to each other, mostly delimiting bone cavities occupied by the bone marrow. The trabeculae are organized in a three-dimensional network whose shape is affected by the mechanical forces that are applied to the bone, this gives the spongy bone tissue a greater resistance to the loads transmitted by the articular surfaces [45].

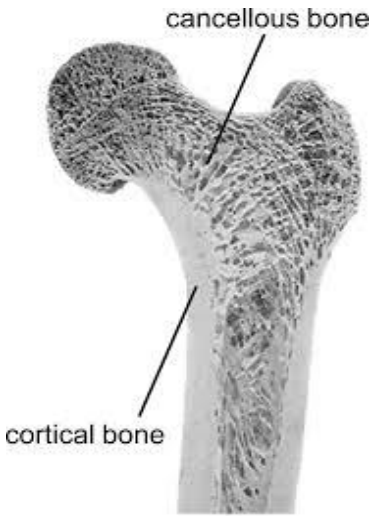

Figure 2.3 – Vertical cut of a human Femur presenting the Corical and Cancellous Bone tissue [47]

The cortical bone tissue consists of cylindrical columns called Haversian systems or osteons.

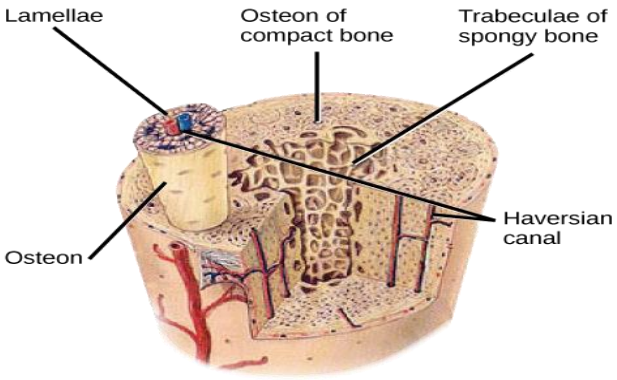

Figure 2.4 - Bone structure, representation of the Haversian System [48]

The Haversian canals are coiled in a spiral and are oriented along the axis of the bone. These canals, located in the centre of the osteons, allow the passage of blood, lymphatic vessels, and the nervous system. The Volkmann canals are positioned transversely to the osteons and connect the Haversian canals to the exterior of the bone [8].

The porosity of the cortical bone is associated with these canals, presenting values between 5% and 10% of the bones volume [45].

When it comes to calcified volume the cancellous bone has values between 80 to 90% while cortical bone has values between 15 to 25%. Thus, the relationship mass/volume is higher in the cortical bone, granting this type bone tissue its higher density and lower porosity, this stands to reason since the resistance of a bone to compression forces is proportional to the square of its density, and the cortical bone is estimated to have a modulus of elasticity and mechanical strength 10 times higher than that of the trabecular bone [45].

On the other hand, the cancellous bone presents 20 times more surface area per unit of volume than cortical bone and thus, its cells are more directly influenced by the cells of the bone marrow. Considering this and its organization, trabecular bone tissue has a greater metabolic capacity and greater remodelling activity and, consequently, a faster response to mechanical, chemical and hormonal stimuli [45].

It is concluded, therefore, that the mechanical specificities already described are a consequence of the different structural characteristics of the two types of bone tissue; it can be affirmed that the cortical bone tissue performs support and protection functions, being located externally in relation to the cancellous bone tissue, which has a metabolic function [8,45].

2.2 - Human body Joints

In the human body a joint is considered to be a point in which two or more bones meet, these joints can be classified as fibrous, cartilaginous or synovial.

Fibrous joints or synarthrodial joints are articulations with only one dense ligament holding it together, this ligament is usually an irregular tissue composed of collagen fibres. Examples of fibrous joints are the teeth and their respective socket as well as the radioulnar and tibiofibular articulations [8,44].

Joints in which the connection between articulating bones is done by cartilage with no synovial cavity are called cartilaginous joints, i.e. vertebrae connections.

Cartilaginous joints are also called synchondroses and symphyses [44]. Synchondroses describe temporary articulations only found on children pre puberty, these include the connections between long bones (i.e. femur and tibia) until they lose their hyaline cartilage [8,44]. Symphyses are joints that permanently possess cartilage and a fibrocartilage pad like the symphysis pubis [8].

Synovial joints are the more common type of articulation on the human body, these joints grant an extreme freedom of movement when compared to the rest [44].

This movement freedom is possible thanks to its synovial cavity and articular capsule that enclose the entire joint [8,44]. The interior of the capsule has a membrane that produces synovial fluid, this fluid is viscous serving as a lubricant to prevent friction it also provides nutrients and removes waste products. This joint also possesses hyaline cartilage that serves as padding for the ends of the articulating bones [44].

Within the synovial joints there are six classifications, these are determined by the shape of the joint and types of movement possible, see figure 6 below.

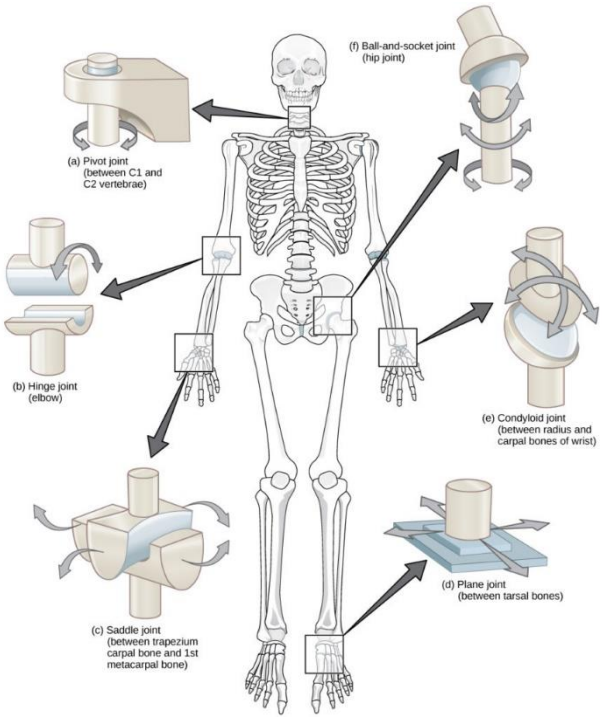

Figure 2.5 – The various types of Synovial Joints in the Human Body [49]

Going with the same order as in figure 6.

First, we have the Pivot Joint, this joint only permits uniaxial movement the movement of one bone around another, an example of this joint is the radioulnar proximal articulation [8,44].

Hinge Joint, has the name implies, only allows movements akin to that of a hinge limiting articulations to flexion/extension movements. In this joint a convex part a bone fits into a concave part of another, examples of this are the elbow and knee articulations [8].

In Saddle Joints and oval surface of one bone fits into a concavity of another bone allowing flexion extension and abduction movements, the carpometacarpal joints of the thumb are an example of this type of joint [44].

Plane joints as the name implies have a flat or slightly curves surface that permit gliding movements (back to front and side to side), this type of joints have their movement restricted in all directions by ligaments, the intertarsal (hand) and intercarpal (feet) joints [8].

Condyloid joints are very similar to Saddle joints the only difference being that Condyloid joints don't allow as great of a movement as the Saddle joints, examples of this joint are the radiocarpal joints [8].

Finally, in the Ball and Socket joints the spherical end of a bone fits into a concave, socket like, part of another bone hence the name. This joint allows for flexion/extension and abduction movements, the hip and shoulder being examples of this type of joint [8].

2.3 - Anatomical Axes/Planes

Anatomical axes and planes have been used for a long time by anatomists not only to describe but also to name many human body parts, therefore it is important to first explain some of these concepts in order to better describe the relative positions and naming of the various parts of the knee joint.

There are three main anatomical planes: the frontal plane which vertically divides the body into its anterior and posterior parts, the transversal plane which divides the body into its superior and inferior parts and the sagittal plane which divides the body into its right and left halves [2,3,7], as shown in figure 7.

These concepts are what gives the name sake to the degrees of freedom of every moving body part, looking specifically at the knee we have 6 different degrees of freedom, movement wise: anterior-posterior, medial-lateral and proximal-distal; and rotation wise: flexion-extension, internal-external and varus-valgus [2,3,7,25,39]; as seen in figure 8 and 9.

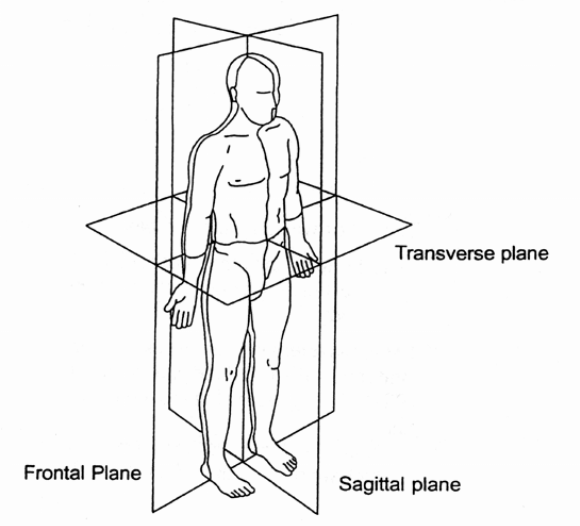

Figure 2.6 – Human body reference planes in anatomical position [50]

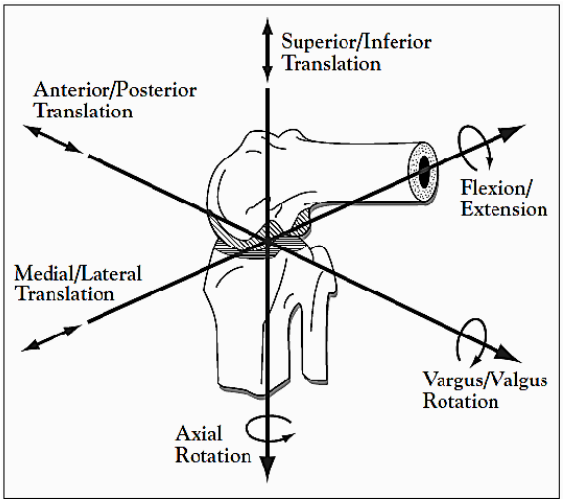

Figure 2.7 – The 6 degrees of freedom of the Knee Joint (3 translations and 3 rotations) [51]

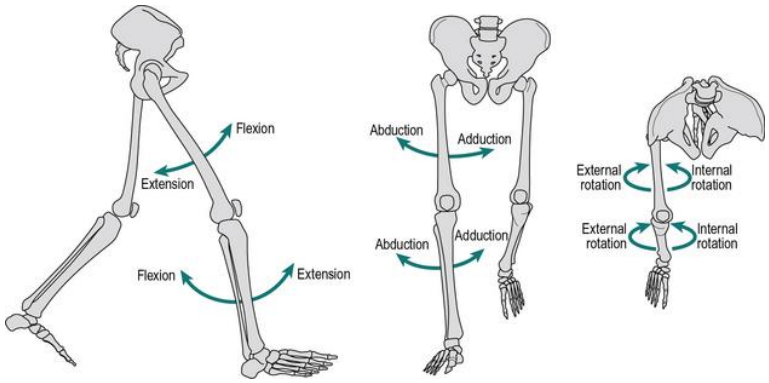

Figure 2.8 – Movements that the Knee Joint enables [52]

Anatomically the knee joint is the interception/connection point of three bones: the femur, the tibia and the patella (covers the anterior part of the knee and is encased in the patellar tendon). An articular cartilage layer covers these bones in the parts in which they connect, in other words the femur is distally covered by this cartilage while the tibia is proximally covered, and the patella is anteriorly covered by it.

Besides the bones, there are the menisci located between the femur and tibia bones, a medial and lateral meniscus, and connecting the femur and tibia, there are the four major ligaments: the anterior cruciate ligament (ACL), the posterior cruciate ligament (PCL), the medial collateral ligament (MCL), and the lateral collateral ligament (LCL).

2.4 - Knee Joint

The Human knee joint, seen in figure 10, is classified as a synovial joint and is one of the most complex joints in the human body, it is composed by bones, ligaments that connect the bones, cartilage, muscles and tendons that attach the muscles to the bone; all of which, in turn, are composed by collagen which is a fibrous protein that is present in connective tissue throughout the body [2-4,8,14,44,53].

Figure 2.9 – Knee Joint Anatomic Components [8]

The knee joint is the structure that links the thighbone (the femur), the lower leg bone (the tibia) and the fibula, the attaching ligaments located on the outer-surface of the knee are the MCL that connect the tibia to the femur and the LCL that connect the fibula to the femur, as for the tendons there is the patellar tendon that attaches the quadriceps muscles of the thigh to the tibia (also being responsible for allowing extension of the knee); inside the joint, between the tibia and the femur, there are two more ligaments the anterior and posterior cruciate ligaments [4,6,8,53].

The knee joint is one of the structures responsible for supporting body weight, during activities like standing, walking and running.

An important characteristic is its capability of providing stability and a wide range of motion (up to 160˚), while lacking strong muscle to support and strengthen it, making it unlike the hip joint, and lacking the strong ligaments that the ankle joint has for support, also being capable of giving some degree of rotation in addition to flexion and extension [1,2,8,10,21,22].

Just like the elbow, the knee joint possesses a hinge joint but compared to the elbow it boasts a far more complex articulation, but the knee joint is much less stable when compared to other joints on the human body; the points of contact for the rounded femoral condyles shift constantly because they roll across the superior surface of the Tibia [4,8,53].

When it comes to the structure, the knee joint, is composed by two joints within a complex synovial capsule; one called tibiofemoral joint, located between the femur and the tibia, and the other called patellofemoral joint, located between the patella and the patellar surface of the femur [8,44,53].

Besides its main structure, the knee joint possesses other components that are crucial for its overall mechanics and should be mentioned [8,44,53]:

- the articular capsule which is strengthened by the tendons that surround the joint;
- the patellar ligament, which extends from the patella to the tibia, and the oblique popliteal ligament which strengthen the anterior and posterior surface of the joint respectively;
- the arcuate popliteal ligament which reinforces the lower lateral part of the posterior surface of the joint;
- The tibial (medial) collateral ligament strengthens the medial aspect of the joint.
- The fibular (lateral) collateral ligament strengthens the lateral aspect of the joint.
- The bursae, saclike structures filled with fluid, help reduce friction.

2.5 - Bones

The knee joint is comprised of three different bones: the femur, the patella and the Tibia, as is possible to see in figure 11.

The femur being the longest bone of the human body is also the heaviest and strongest bone, covering the length of the entire thigh, it articulates proximally to the hip bone and extends distally to articulate with the tibia [8,44,53]. This bone is responsible for bringing the knee joint closer to the medial line of the body (centre of mass line) thanks to it bending medially, the bending is more pronounced on females because of the broader pelvis [53].

The head of the knee articulates with the acetabulum in order to form the hip joint, the neck of the knee, right below the head, is a constricted area that helps with the weight sup-

port [53]. The femur prolongs into the medial and lateral condyles distally, which in turn articulate to the tibia [4,53].

The patella or kneecap, as is most commonly called, is a sesamoid bone [44] located between the tibia and femur. This bone has a round and flat shape and is a lot smaller when compared to the other two [8], see figure 11. The patella's functions are to increase the leverage of the tendon and maintain its position when the knee is flexed and protect the knee joint [53].

During flexion of the knee the patella moves according to the movement; tracking/gliding up or down, depending on the phase of the movement, in the groove between the two femoral condyles [53].

The tibia, just like the femur, is one of the largest bones in the human body being another weight bearing bone in the leg [4,8,44,53]. The tibia articulates proximally to the femur in the knee joint. In its anterior surface below the condyles there is the tibial tuberosity, which is the point of attachment for the patellar ligament [8], and distally on its medial surface the tibia, forms the medial malleolus which articulates with the talus of the ankle forming the protrusion that we all have on the medial surface of our ankle [8,53].

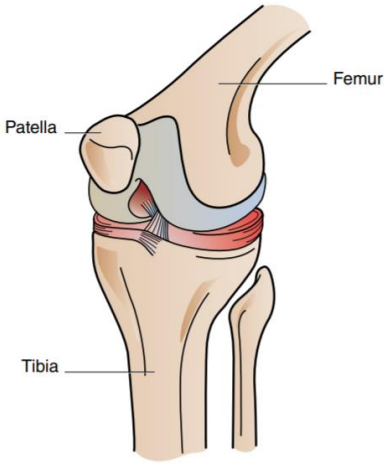

Figure 2.10 – Bony Components of the Knee Joint [53]

2.6 - Menisci

The meniscus is a component vital for the normal function and longevity of the knee joint, this knee component is composed by a dense extracellular matrix, which in turn is composed of water (72%) and collagen (22%) [54]. It is located between the femur and tibia in the "joint space" [4,8,44,53,54].

The menisci have a number of roles but the most important one is, through congruency, to transmit load across the tibiofemoral joint in order to significantly decrease the stress that the articular cartilage is under [21,53]; besides this the menisci is also responsible for providing joint stability, shock absorption, nutrition, lubrification and proprioception to the knee joint [21,54,55].

The meniscus is shaped like crescent edges of cartilage located medially and laterally in the knee, see figure 12, these occupy roughly one-half to two-thirds of the joint space [54];

the outer, thicker convex, section of the meniscus is attached to the knee joint capsule while the inner, thinner concave, part isn't attached at all [54]. The menisci possess a meniscal horn that connect them to the subchondral bone of the tibial plateau, these ligaments also serve as means of transmitting sheer and tensile loads to the bone and also serve as a means to decrease the contact area [21,54,55].

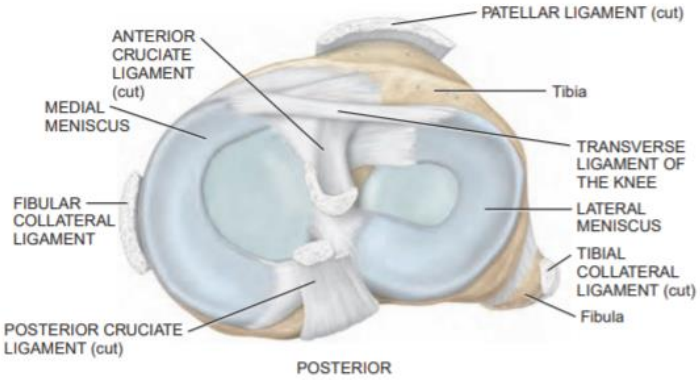

Figure 2.11 – Superior view of the Menisci [53]

The medial meniscus is C shaped and occupies 60% of the articular contact area, the attachment site of its anterior horn may vary into either a soft tissue or a firm bony site, with this last one being more common [54]; the posterior horn always attaches to the tibia, anteriorly to the PCL attachment site [54].

The lateral meniscus is almost circular shaped and is smaller than the medial meniscus but considerably more mobile, its anterior horn attaches to the tibia posteriorly and laterally to the ACL insertion site, the posterior horn attaches between the insertion sites for the PCL and the posterior horn of the medial meniscus [54].

As the femur, when the movement requires, compresses the Tibia the menisci is compressed within the joint cavity, it deforms to conform with the femoral condyle allowing for a better weight distribution through a larger area and decreases the stress exerted on the tibia [21,26,54].

Biomechanical studies have demonstrated that 40% to 60% of any given load applied on the knee joint is transmitted to the menisci [54].

The menisci are also capable of moving radially outward and posteriorly with the knee flexion, in order to follow the rolling and sliding of the femoral condyle with flexion, during radial deformation the menisci is fixed by its posterior and anterior horns [54].

2.7 - Articular Cartilage

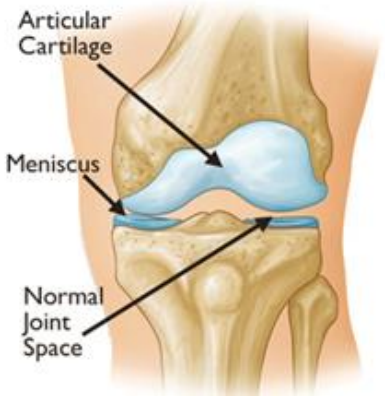

Figure 2.12 – Articular Cartilage in the Knee Joint, adapted from [56]

The knee joint, like any other synovial joint, has articular cartilage more specifically at both ends of the femur and tibia involved in the joint and on the posterior side of the patella, as it is possible to see in figure 13 [4,8].

Articular Cartilage is named so because of how the bones, when moving against each other, articulate [4].

Articular cartilage is the type that exists in bigger quantity in the human body [53], it is composed by hyaline cartilage and is usually found covering part of the epiphyses of a bone that forms an articulation with another bone [8,53], it affords flexibility and support.

It also, with the help of a thin layer of synovial fluid, reduces friction and wear between the moving bones; and absorbs shock in the joints by spreading the load over a wider area with the objective of reducing the amount of stress at any given point but because it lacks perichondrium, self-repair is very limited [4,8,53].

2.8 - Ligaments

Unlike a ball joint, like the hip joint, which is socketed into a deep pocket, the knee joint behaves more like a hinge [4,8,44,53], being structured to mostly move in one plane, not having significant protection against trauma or stresses. Therefore, in order to compensate for this, the knee joint possesses strong knee ligaments [4].

These ligaments are responsible for controlling and limiting knee hyperextension, varus/valgus stresses, anterior/posterior displacement of the tibia, rotatory stabilization (prevention of anteroposterior displacement/rotation of the tibia) and provide general stability to the knee by constantly being in a state of in situ stress when no muscles or tendons are being exerted [2,3,4].

It is important to note that the anatomical position and geometry of each ligament determine the direction in which the ligament is capable of operating [2,57].

The knee possesses 4 main ligaments, as seen in figure 14, that have already been mentioned previously, namely: the ACL (Anterior Cruciate Ligament), the PCL (Posterior Cruciate Ligament), the MCL (Medial Collateral Ligament) and the LCL (Lateral Collateral Ligament).

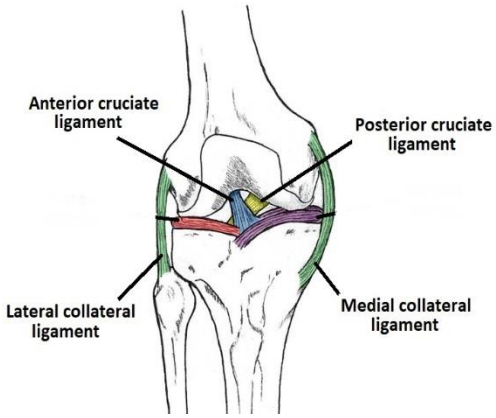

Figure 2.13 – Anatomical position of the four major Knee Ligaments, adapted from [58]

Each ligament performs a different role in the joint. The cruciate ligaments, ACL and PCL, are intracapsular and extra synovial ligaments that handle front-to-back movements while ensuring stability by not allowing the Tibia to slide forwards or backward in relation to the Femur during flexion and extension of the knee as well as not allowing hyperextension [4,7,59]. The MCL and LCL handle the side-to-side movements, strengthening the articular capsule medially and laterally as both their names implies [4,7,57,60].

Besides these four major ligaments there still other ligaments in the knee joint crucial for the overall stability and mechanic of the knee. These are Humphrey and Wrisberg ligaments located anteriorly and posteriorly to the PCL respectively, the oblique and arcuate popliteal ligaments both of which posteriorly cross the knee and transverse ligament that connects the menisci between the femur and tibia [4,8,44,53].

Anatomically these ligaments are short bands of fibrous connective tissue composed by collagen fibre [2-4,53] bundles as seen in figure 15, water (65% to 70% of its weight) [2,3] and proteoglycans which provide lubrification and spacing [2,3]; these bind the bones across the joint, generally serving to guide joint motions and prevent irregular motion movement [2-4,12,53].

As mentioned previously, these ligaments are composed by bundles of collagen fibres, but it is important to specify the different types of collagen it possesses and their role: the major types are collagen type I (70% to 80% of ligaments dry weight) responsible for the ligament's tensile strength, collagen type III (8% dry weight) and type IV (12% dry weight), other collagen types that have been found are II, IX, X, XI and XII but at a really small quantity (less than 1% dry weight)[2,3].

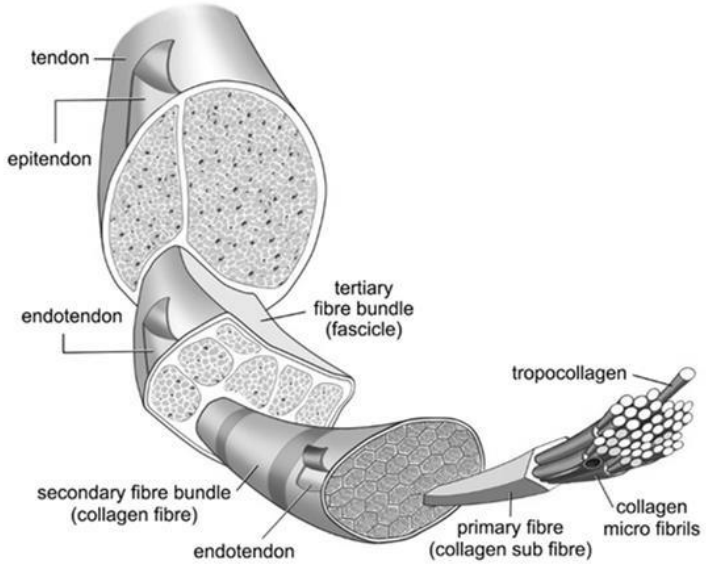

Figure 2.14 – Ligament and Tendon composition, adapted from [60]

The collagen micro fibrils are compressed in various forms in the ligaments in order to make it easier and faster to recruit when the movement requires more to resist the increased load or when subjected to varying tensile forces. Besides this, their compressed nature also serves to guide joint motion and restrain it in extreme cases.

The collagen fibres, when in tension, react by elongating, i.e. in normal day to day activities, this serves to help maintain the normal kinematics of the joint allowing for easier and smoother joint movement but when it becomes "excessive" the collagen fibres will increase their stiffness in order to restrict the movement. However, if the tension exceeds what the fibres are capable of handling the risk of tearing/damage on the ligament increases. [2,3,4,8]

These ligaments may present different anchor types on their respective bones depending on the insertion, there is direct and indirect insertion.

In direct insertion, the fibres insert directly in the bone and the transition of ligament to bone occurs in four zones: ligament, fibrocartilage, mineralized fibrocartilage and bone. While indirect insertion is characterized by a superficial and deeper layer of fibres with the first connecting with the periosteum and the later connecting with the bone at acute angles via "Shapey's fingers". A ligament that presents both direct and indirect insertion is the MCL, it has a direct femoral insertion and an indirect tibial insertion [2,3].

As mentioned, ligaments are suited to transfer loads from bone to bone along its longitudinal direction and that's the main reason why these are studied through uniaxial tensile tests in a bone-ligament-bone complex which result in a nonlinear load-elongation or stress-strain curve, like the ones in figure 16 below [2,3].

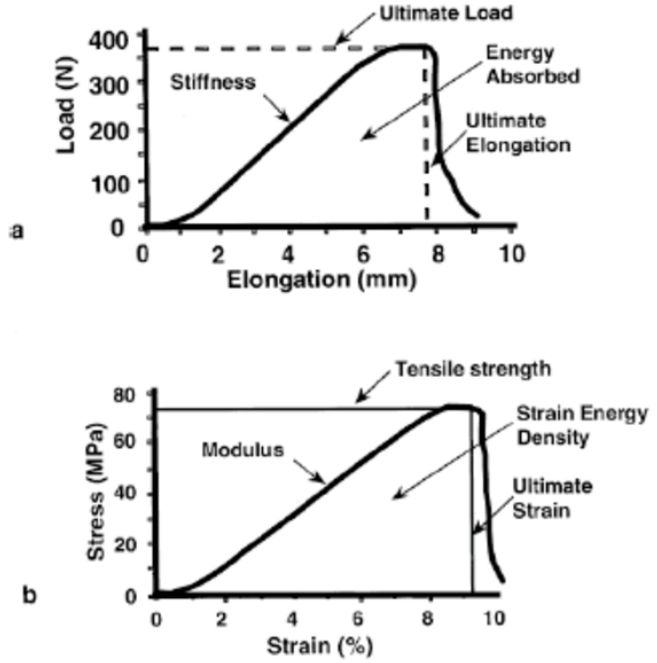

Figure 2.15 – a) Ligament Load-Elongation Curve, b) Ligament Stress-Strain Curve, adapted from [2]

A load-elongation curve, figure 16 a), is non-linear and concave upward [3] used to describe the physical and structural properties that define the behaviour of a given ligament. The information attainable from these curves are the stiffness, ultimate load/elongation and the energy absorbed by the ligament [2,3].

The stress-strain curve, figure 16 b), is obtained using the load-elongation curve when the length and cross-section of the ligament are known. With this curve it is possible to attain the modulus, tensile strength, strain energy density and ultimate strength [2,3].

These tests show that the mechanical properties of the various ligaments depend on environmental factors, the geometry of the ligament and the collagen bundle distribution within the ligament [2,3]. This last one implying that the contribution from each bundle may be different to the overall joint stability, which may be affected when they're replaced. [2]

The four major ligaments will be described in more detail in the next sections.

2.8.1 - ACL

Characterization of the ACL mechanical properties is a big challenge, difficulties associated with finding completely unloaded conFiguretions of the ACL that coincide with physiological relevant ones, as well as, getting the shape structure and orientation of the ACL correctly make this a challenge [7].

The ACL originates from a connection to the posterior part of the medial surface of the lateral femoral condyle, this connection being oval in shape and occupying an area of 2 cm^2 [7,8,53].

This ligament, as the name implies, courses anteriorly but also courses medially and distally from the femur to the tibia where it inserts over an area of 3cm^2 on the tibial spines [7],

this part of the ligament that is attached to the tibia is substantially wider and stronger when compared to its other end [7,8,53].

At the tibial insertion, the ligament passes below the transverse meniscal ligament, where it is believed that some fibres of the ACL blend with the fibres of the anterior attachment of the lateral meniscus though the relevance of this blending hasn't been discovered [7].

Interestingly, the cross-section area of the ACL varies along its length, with its smaller value being located at the mid-substance. The functional reason for this area variation, is to minimize stress concentrations in the interface between ligament and bone [5,53].

This is also the reason why adult ACL injuries are mainly located in the mid-substance area; it also explains why children ACL injuries appear primarily on the bony avulsions, where modulating and weaker ligament to bone interface exists [7].

Another interesting aspect is that the ACL size also varies depending on sex, with male ACL being thicker, wider and longer [7,11]; this difference only starting to be noticeable after the development and growth spurt [7].

Within the ACL there are two discrete bundles: the anteromedial bundle (AMB) and the posterolateral bundle (PLB) [6,7,22,25]; these two structures possess unalike spatial and mechanical properties [7]. Anatomically these two bundles intertwine with each other between their respective insertion points, in which each occupies 50%, with AMB being longer compared to PLB [7].

Referring now to the insertion sites, the AMB inserts posteriorly and superiorly to the femur and medially to the tibia, and conversely the PLB inserts anteriorly and inferiorly to the femur and laterally to the tibia [7]. These bundles have been observed to have reciprocal tensioning pattern during their function in passive flexion and extension movements of the knee joint, with AMB (29 mm–35 mm) observed to be tauter in flexion and the PLB (18 mm–26 mm) in extension [7].

2.8.2 - PCL

The Posterior Cruciate Ligament (PCL) is the largest and strongest intra-articular ligament in the knee joint, it is attached to the tibial spine distally and crosses the knee joint attaching its other end to the lateral aspect of the medial femoral condyle; it is reported that its femoral attachment can be twice the size of its tibial attachment (112 to 118 mm^2) [59].

The PCL, just like the ACL, is comprised of two bundles, the larger one being the anterolateral bundle (ALB) and the smaller one being the posteromedial bundle (PMB); but, to differentiate it, the PCL has an inclination angle more horizontal when compared to the ACL, which has a more vertical angle when in full extension, the same comparison can be made to their femoral insertions with PCL's insertion being more horizontal and the ACL's being more vertical; the PCL also has a cross section larger than the ACL [59].

Mechanically the PCL has the role to restrain posterior tibial translation at all flexion angles, with both bundles (ALB and PLB) playing significant roles in maintaining knee stability in case the other bundle fails to respond, suggesting a co-dominant relationship between them [59].

2.8.3 - MCL

The Medial Collateral Ligament (MCL) is one of the four major ligaments in the knee joint, it has a length of 8 to 10 cm being the largest structure in the medial aspect of the knee joint.

The MCL is comprised by two components: a superficial and a deep component. The superficial MCL component, also named tibial collateral ligament, originates from the posterior aspect of the medial femoral epicondyle and connect distally to the medial condyle of the tibia below the joint line near the level of the pes anserinus insertion, this component is acts as the primary static stabilizer for valgus stress in the knee. The deep MCL component, also named mid-third capsular ligament, is divided into meniscofemoral and meniscotibial and is responsible for restraining anterior translation movement of the tibia, with a secondary role in static stabilization for valgus stress [57].

2.8.3 - LCL

The Lateral Collateral Ligament (LCL) is a ligament considered to be a component of the posterolateral corner, it runs from the outer surface of the lateral condyle, posteriorly and obliquely inferiorly, to the fibular head; since the LCL is outside the capsule throughout its length it is considered an extracapsular ligament [61].

The LCL is majorly responsible for passively stabilizing the lateral aspect of the knee as well as restraining varus stress at the knee joint (mainly at 0 to 30-degree of knee flexion); secondarily it also serves as restraint for tibial external rotation, most optimally with the knee at full extension when the ligament is under greatest force, helping the popliteus tendon, popliteofibular ligament, and posterolateral capsule which are the primary static restraints.

The LCL is also capable, to a lesser degree, of restraining varus forces at additional flexion ranges and adding stability to tibial internal rotation [61].

Chapter 3

Common Injuries and Treatments

Knee injuries are most common on sports [7,10,13,63] accounting with 15% to 50% of all sports injuries, mainly those in which high stress is focused on the legs; among these the sports with higher knee injury rate are: soccer, ice-hockey, volleyball, basketball and judo [10]. By looking at insurance data on licensed competitors, in Finland, showed that in knee injuries 21% happened in soccer, 20% in judo, 19% in volleyball, 17% in ice-hockey, and 16% in basketball, with the remaining 7% being distributed between other sports [10].

The cost of knee injuries representing a major part of expenditure for medical care of sport injuries, the reason being the long and costly rehabilitation and the possibility of impairment (to various degree) [4,14].

As mentioned previously, athletes that practice these sports exert tremendous stresses on their legs and knees; normally the medial, lateral ligaments and meniscus shift their position, depending on the movement, while performing high stress activities when the knee is partially flexed, the meniscus may be trapped between the femur and tibia resulting in a tear of its cartilage [3].

Most commonly, for the injurie to occur, the lateral surface of the leg is driven medially, either because the movement was performed incorrectly (on a fall) or because of an external interaction (a tackle by a different athlete), tearing the medial meniscus; this type of injurie besides being quite painful, the torn cartilage causes restriction to the movement of the joint also leading to chronic problems and the possible development of “trick knee”, instability of the knee. [3,7,10]

Other knee injuries happen involving the tear of the supporting ligaments or damage of the patella. Rupture of the ACL is a common injury [7,10,13,62], which affect more women than men [3,7,10,11] (two to seven times more [8]), with a study revealing that during the activities of ‘‘Youth and Sports’’ (an organized sports and recreation event for Swiss youth) females were significantly more at risk in six sports: alpinism, downhill skiing, gymnastics, volleyball, basketball and team handball [4].

This type of injurie tends to happen when, during movement, the weight bearing knee twists [8].

When an ACL injury is suspected the normal clinical procedure is to, firstly, use the Anterior Drawer and Lachman tests in order to assess the severity of the injury [2,4,22,63]. These tests consist in the anterior displacement of the tibia by applying a translational load and

manually flexing at 90˚ to 30˚, while the femur is fixed; the objective here is to measure the laxity of the injured joint compare it to a healthy one [2,63].

3.1 - ACL Tear Treatment techniques

As previously mentioned, ACL injury is very common, with 80% of knee-based surgeries being performed on the ACL [13,63], one of the major problems with complete rupture of the ACL is that besides leading to incomplete healing it also causes insufficient vascularization.

Reconstruction of the ACL is the more popular method to treat these injurie, it aims to reinstate stability to the knee and preventing further damage be done to the menisci, it also reduces the danger of osteoarthritis developing.

Advancement, as led to the creation of the arthroscopic anatomic grafting techniques which consist in grafting tissue (organic or synthetic) to the damaged ACL area.

A considerable number of different graft types exist, but generally speaking, all grafts can be organized into three types: autologous grafts, allografts, and synthetic ligaments [13].

An example of autologous grafts is hamstring and bone-patella tendon grafts, these grafts have the advantage of providing a strong scaffold for in-growth of collagen fibres with minimal risk for body rejection of the grafts. But a major disadvantage is the risk of harvest site morbidity that it may cause making a long period of rest, and avoiding any kind of straining activities, necessary for revascularization. This period lasting up to 12 months [13,63,65].

On the opposite spectre, there are the allografts which have the advantage of having low risk for harvest site morbidity but are prone for graft rejection. These have high potential to cause a viral infection, have a slower healing process and higher failure rates making them a very rare choice [13].

As for synthetic ligaments, the option for using synthetic biomaterial to reinforce these grafts has been in development since the 1980's, these reinforced grafts were developed to have increased strength and stability, immediately post operation, to reduce harvest site morbidity and eliminate potential disease transmission [13,66].

But even though these were the objectives, the first synthetic ligaments were mostly failures being associated with the development of synovitis.

Nowadays, with the advancement of technology, there has been development of new kinds of synthetic ligaments with one of them gaining popularity, Ligament Advanced Reinforcement System (LARS) [13,67].

LARS is a non-absorbable synthetic graft made out of terephthalic polyethylene polyester fibres (PET) [67].

PET is a semi crystalline thermoplastic polymer widely used all over the world, being better known in the textile industry as "polyester". This polymer is a naturally transparent, strong and lightweight plastic used more commonly as fibre for clothing, packaging for various foods and beverages and as an engineering plastic that, when combined with other materials, strengthens them [68,69]. It is produced from the synthesis ethylene glycol and terephthalic acid which are held together by a polymer chain.

The main characteristics that define PET are its chemical resistance not reacting with water or organic tissue, its strength to weight ratio, it is a material that is readably available at a relatively inexpensive cost and it is shatterproof. All these characteristics make this a promising material for synthetic ligament grafts, but it does have its drawbacks, unfortunately PET

is not biodegradable which means that it will stay within the recovered ligament indefinitely [1].

LARS possesses a scaffold which consists of multiple fibres parallel to each other at 90° angles, this design was chosen in order to prevent fibre breakdown which was a problem in previous graft designs made from woven materials, furthermore it's believed that the LARS design, during movement, facilitates tensioning of the graft fibres [13].

And just like the others, this graft aims to provide a base for the injured ligament to heal and repair itself.

Figure 3.1 – Ligament Advanced Reinforcement System [70]

Surgically, LARS, uses an intra operative intensifier X-ray system to position the tunnels for the graft through the ACL, this makes it so the synovial lining and the ACL fibres are left in place, resulting in reduced trauma to the soft tissues and reduced surgery time [71]. This is an advantage over the traditional ACL reconstruction techniques since, in order to visualize and position the graft, it is required that the torn ACL fibres and synovial lining be debrided [13].

Generally, the LARS graft technique aims to optimise reconstruction of the ACL fibres by providing a scaffold for tissue ingrowth, while preserving some vascular proprioceptive nerve supply and mechanical stability.

LARS also boasts the ability to promote fibroblastic in growth and low probability to produce synovitis.

This last claim being contested. One study performed by Batty et al supports this claim, chowing a rate of failure with values as low has 2.6% for the LARS grafts [72]; and others like Gao et al, Glezos et al and Li et al [73,74,75] reporting that synovitis can happen and is associated with cases in which complete graft failure is verified.

Chapter 4

Knee Biomechanics and Kinematics

Kinematics, when applied to the human body, represent the motion, locomotion and gait of diarthrodial joints [2]. The information that we can take from analysing the Biomechanical/Kinematic characteristics of the various joints is valuable to obtain a dipper knowledge on them: knowing how they function during normal movement is important material used for comparison purposes when diagnosing injury and checking for the success of treatment [2,3].

Specifically, for the knee, examination of the injured joint is performed by analysing the knee motion and comparing it to that of a non-injured one [2], the Lachman and drawer tests are an example of this [2,4,22,39]. What the examiner looks for, in these tests, is excess motion in a direction from the injured knee, the direction in which excessive motion happens is related to the damaged component within the knee [2].

The function of the knee and its components is to prevent over elongation during normal movement activities, either rotational, translational or both [1,2,8,10,22,63]. In order to better understand knee joint kinematics, it is important to study their behaviour. The knee joint movements are only possible through its ligaments, other soft tissues and the articular surfaces [2,4,7,57,59,62].

The knee has six different degrees of freedom, three rotations and three translations [2,3,7,14,39]. As for its planes of motion the knee possesses three main axis: the tibial shaft axis, the epycondral axis and the anteroposterior axis [2]; the translations along these axis are, respectively: proximal-distal, medial-lateral and anterior-posterior; and the rotations along these axis are, respectively: internal-external, flexion-extension and varus-valgus, all of this can be seen in the figure 18 bellow [2].

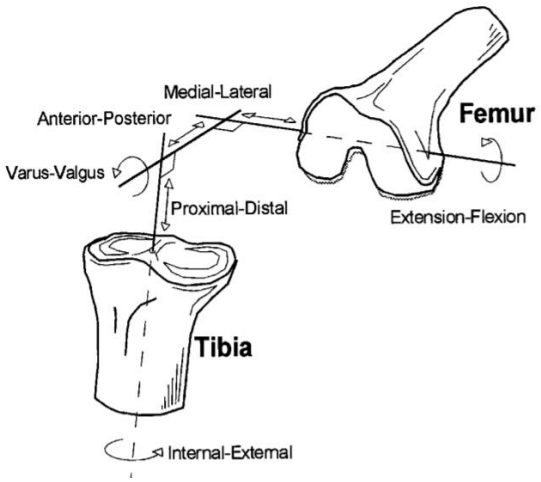

Figure 4.1 – The six degrees of freedom of the Human Knee Joint [2]

As it is known the main plane of rotation for the knee joint is flexion-extension in the epycondral axis with smaller ranges of motion both in the other axis [76]. The range of motion in the epycondral axis varies between 130° and 140°, in passive motion, and 5 to 10°, in hyperextension. As for the tibial shaft axis and anteroposterior axis the combined range of motion, in internal-external rotation and minimal valgus-varus rotation is within the active and passive ranges of approximately 70°. It's important to note that these values vary depending on the degree of flexion and extension of the knee, with the ranges of internal-external rotation being maximal and minimal at the values of 0° and 90° of flexion respectively [76,77].

As mentioned previously the normal motion and kinematics of the knee joint is only possible because of its many components and if one of them is damaged the entire motion of the knee will likely be altered [2]. For example the complete rupture of one of the ligaments will cause joint instability which in turn will increase the stress other components, like the menisci or the articular cartilage, will be put under in order to compensate for the ligament, resulting in these components getting damaged as well further destabilizing the joint.

Chapter 5

Methodology

5.1 - Finite Element Method (FEM)

The Finite Element Method, in the engineering field, has the objective of determining the stress and strain states of an object with arbitrary geometry in which forces are being applied externally. It is a powerful numerical method, devised for analysis of various engineering problems, from the more elementary to the more complex, it being capable of handling geometrical complexity, a large array of boundary conditions, nonlinearities and coupled phenomena [78].

There are, nowadays, a large number of licensed computer software that use this method like Femap, MATLAB, MFEM, Abaqus, etc, that have made it a “regular use” tool in the engineering research field.

The FEM is the numerical technique used for Finite Elements Analysis (FEA), which is used for this study.

In order to run a FEA, the first step is to divide the structure as a whole into smaller parts, this is done by creating a mesh. This mesh will contain a large number of elements that will make up the general shape of the model, the reason for this is to transcribe the complex shape of the model into a series of, comparably, simpler mathematical points. [78, 79]

The second step is to try and find the solution closest to reality for each finite element, this solution will be a linear combination of nodal values and approximation functions. Finally, with the data from each element it is possible to obtain the solution for the whole structure [78]. Interpolation may occur, since some nodal points might be shared by different elements, but these approximations are within what is expected [79].

But before implementing a FEA and even meshing the model, first it needs to be categorized by its structure. This is done by classifying it according to its geometry, material type and applied actions.

Geometry wise the model needs to have a well thought out node and element definition, this is done through correct node/element number and coordinate assigning, defining individual nodes/elements or grouping them into sets accordingly.

For the Material, in order to be able to start a FEA a material type needs to be assigned to the elements of the model. Most, if not all, CAD programs have a material library to choose from as well as a means to create a custom type of material for analysis.

Applied actions pretrains to the constraints and interactions that the model will be under during analysis.

Another consideration is the inherent simplifications that will have to be done to the model in order to achieve a balance between results and computing processing power, the application of the FEM will vary depending on the level of complexity.

The main aspects to have in consideration before applying the FE model in structure analysis are [78]:

- Whether the Analysis is Dynamic or Static - The consensus is that the actions applied on the structure are all generally dynamic, and that there is inertia associated to the acceleration to which every single part of the structure is under. But this does not mean that every situation should be considered as having dynamic behaviour, in some situations the inertia is negligible, this results from the applied actions having low values; in these cases, the analysis is considered static.

- Whether the Analysis is Linear or Non-Linear - Generally speaking, in an analysis of a solid body in which the displacements are small (when compared to the elements of the structure), it is said that there is no influence on the stress and tension distribution by the geometry modification, and therefore the entire analysis is performed with the initial unmodified geometry classifying this as a Linear Analysis. If the opposite happens, i.e. the body suffers considerable deformation influencing the stress and tension distribution, then it will be classified as a Non-Linear analysis.

The next parts will show in some detail the formulation of the FE methodology and some other concepts associated with it, for more detailed information on the subject the reader is referred to read the original document [78].

5.1.1 - FEM Fundamentals

The formulation of the FEM requires the existence of an integral equation, in other words the basis of this method is an integral equation. This integral will be converted over a complex domain, of volume V, for a sum of integrals extended to subdomains of simple geometry, of volume Vi.

This next equation (1) illustrates an example of this, which corresponds to the integral volume of a function f.

$$\int_v f\, dV = \sum_{i=1}^{n} \int_{vi} f\, dV\,. \tag{1}$$

On equation (1) it is assumed that

$$V = \sum_{i=1}^{n} Vi\,. \tag{2}$$

By calculating all the extended integrals to the subdomains Vi, there only is the need to calculate the sum corresponding to the second part of equation (1) to obtain the extended integral of the entire domain. Another aspect to note is that each subdomain Vi coincides with an element of the structure with simple geometry.

5.1.2 - Gauss Quadrature

The integral calculations needed to attain when using Finite Element Method are very complex, for example the primitive function does not exist or is not explicit making it very difficult to establish and apply. Therefore, the application of numerical integration or Gauss Quadrature technique is essential.

To explain this technique an example, is presented below.

Integration of a Polynomial Function

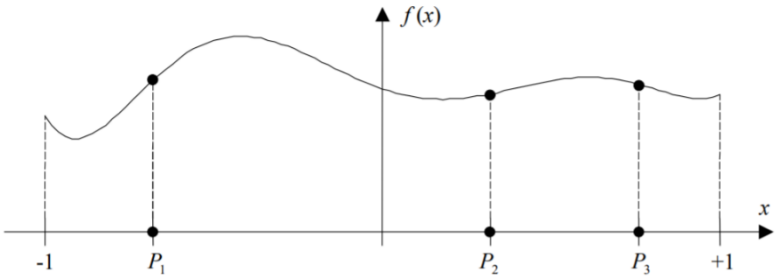

$$f(x) = c_0 + c_1x + c_2x^2 + c_3x^3 + c_4x^4 + c_5x^5. \quad (19)$$

In order to explain how the integration of a polynomial function generically works a simple degree 5 polynomial function is presented.

The integral of function (19) in the interval presented is

$$I = \int_{-1}^{+1} f(x)\,dx = \int_{-1}^{+1} (c_0 + c_1x + c_2x^2 + c_3x^3 + c_4x^4 + c_5x^5)\,dx \quad , \quad (20)$$

$$I = 2c_0 + 0c_1 + \frac{2}{3}c_2 + 0c_3 + \frac{2}{5}c_4 + 0c_5 \quad . \quad (21)$$

Now, to avaluate the integral of f(x) the next step needed to take is to sum the estimated values of f(x) in specific points, P1 P2 and P3 in this example, and multiply each of them by their respective weights (Wi). This integral is represented next (22), and is designated as J:

$$J = W_1\,f(P_1) + W_2\,f(P_2) + W_3\,f(P_3) \quad . \quad (22)$$

Looking at (19), (22) becomes

$$J = W_1\left(c_0 + c_1P_1 + c_2{P_1}^2 + c_3{P_1}^3 + c_4{P_1}^4 + c_5{P_1}^5\right)$$

$$+ W_2 \left(c_0 + c_1 P_2 + c_2 {P_2}^2 + c_3 {P_2}^3 + c_4 {P_2}^4 + c_5 {P_2}^5\right) + W_3 \left(c_0 + c_1 P_3 + c_2 {P_3}^2 + c_3 {P_3}^3 + c_4 {P_3}^4 + c_5 {P_3}^5\right) , \quad (23)$$

or

$$\begin{aligned} J = {} & (W_1 + W_2 + W_3) c_0 + \\ & + (W_1 P_1 + W_2 P_2 + W_3 P_3) c_1 + \\ & + \left(W_1 {P_1}^2 + W_2 {P_2}^2 + W_3 {P_3}^2\right) c_2 + \\ & + \left(W_1 {P_1}^3 + W_2 {P_2}^3 + W_3 {P_3}^3\right) c_3 + \\ & + \left(W_1 {P_1}^4 + W_2 {P_2}^4 + W_3 {P_3}^4\right) c_4 + \\ & + \left(W_1 {P_1}^5 + W_2 {P_2}^5 + W_3 {P_3}^5\right) c_5 + \end{aligned} \quad (24)$$

Since it is intended, in this example, that (24) be equal to (21).

$$I = J , \quad (25)$$

and we get:

$$\begin{aligned} & 2c_0 + 0c_1 + \frac{2}{3} c_2 + 0c_3 + \frac{2}{5} c_4 + 0c_5 = \\ & = (W_1 + W_2 + W_3) c_0 + \\ & + (W_1 P_1 + W_2 P_2 + W_3 P_3) c_1 + \\ & + \left(W_1 {P_1}^2 + W_2 {P_2}^2 + W_3 {P_3}^2\right) c_2 + \\ & + \left(W_1 {P_1}^3 + W_2 {P_2}^3 + W_3 {P_3}^3\right) c_3 + \\ & + \left(W_1 {P_1}^4 + W_2 {P_2}^4 + W_3 {P_3}^4\right) c_4 + \\ & + \left(W_1 {P_1}^5 + W_2 {P_2}^5 + W_3 {P_3}^5\right) c_5 + \end{aligned} \quad (26)$$

and considering that c_i values are in both branches of equation (26) for the equality to exist we can consider that:

$$\begin{cases} W_1 + W_2 + W_3 = 2 \\ W_1 P_1 + W_2 P_2 + W_3 P_3 = 0 \\ W_1 {P_1}^2 + W_2 {P_2}^2 + W_3 {P_3}^2 = 2/3 \\ W_1 {P_1}^3 + W_2 {P_2}^3 + W_3 {P_3}^3 = 0 \\ W_1 {P_1}^4 + W_2 {P_2}^4 + W_3 {P_3}^4 = 2/5 \\ W_1 {P_1}^5 + W_2 {P_2}^5 + W_3 {P_3}^5 = 0 \end{cases} . \quad (27)$$

Then by solving (27) as a system of six equations with the objective of discovering P_1 P_2 P_3 and W_1 W_2 W_3, we get:

$$\begin{cases} P_1 = -\sqrt{3}/\sqrt{5} = 0.77459\ 66692 \\ P_2 = 0 = 0 \\ P_3 = \sqrt{3}/\sqrt{5} = 0.77459\ 66692 \\ W_1 = 5/9 = 0.55555\ 55556 \\ W_2 = 8/9 = 0.88888\ 88889 \\ W_3 = /9 = 0.55555\ 55556 \end{cases} . \quad (28)$$

Finally, the integral value of a degree 5 polynomial can be obtained with:

$$I = J = \frac{5}{9} f\left(-\frac{\sqrt{3}}{\sqrt{5}}\right) + \frac{8}{9} f(0) + \frac{5}{9} f\left(\frac{\sqrt{3}}{\sqrt{5}}\right) . \quad (29)$$

5.1.3 - Unidimensional Finite Elements

In order to better understand the FEM when applied to 2D and 3D regular problems, it is a good idea to exemplify the one-dimensional application of it, since it is simpler to explain and understand even though it has very little practical interest.

The FEM is based on displacement methods and discretization of a structure in sub-structures. These substructures are called finite elements and they have a known behaviour and number of nodes, the displacement is measured using the general displacement of these nodes, and the displacement of the rest of the points in the structure is measured by interpolating the nodes displacement.

Now, to demonstrate the general resolution of one of these one-dimensional problems in which the objective is to find the displacement on a finite element, consider the example figure 19 below (note that the only relevant axis in this example is x):

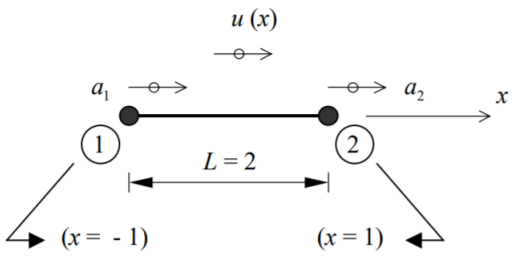

Figure 5.1 – Unididmensional Finite Element with two nodes [78]

For this example, we have an element composed by two nodes (node 1 with x=-1 and node 2 with x=1).

Equation 12, below, represents the displacement field of the element.

$$u(x) = \begin{cases} u(-1) = a_1 \\ u(+1) = a_2 \end{cases} \quad , \tag{12}$$

with a_1 and a_2 representing the value for the displacement of nodes 1 and 2, respectively.

Now if we regard the displacement variation between nodes 1 and 2 as linear, we get the following function:

$$u(x) = \frac{a_1+a_2}{L} + \frac{a_1-a_2}{L} x \quad . \tag{13}$$

This way, in 13, u(x) is linear in x and respects 12, accurately representing the displacement field of the element.

By placing a_1 and a_2 separately and writing 13 in a matrix form, as seen in equation 14, we can represent 13 in a more simplified (equations 15).

$$u(x) = \left[\frac{1}{2} - \frac{1}{L}x \quad \frac{1}{2} + \frac{1}{L}x\right]\begin{bmatrix} a_1 \\ a_2 \end{bmatrix} \quad <=> \quad u(x) = [N_1(x) \; N_2(x)]\begin{bmatrix} a_1 \\ a_2 \end{bmatrix} \quad , \tag{14}$$

$$u = \underline{N}\,\underline{a} \quad . \tag{16}$$

5.1.4 - Virtual Work Principle

The virtual Work Principle or Virtual Displacement Principle is a concept that is associated with FEM.

It establishes that, the work performed by the external forces in the virtual displacement of the points in which they are applied, is equal to the work performed by the internal strain in the virtual deformation of the body. In simplified terms, the external virtual work corresponds to the sum of the internal virtual work.

$$External\,Work = Internal\,Work \quad . \tag{17}$$

In this context the word “virtual” means that the displacement and the force values may not correspond to each other, but the force values are static while the displacement values are cinematic.

Virtual displacement describes any non-verifiable displacement, in other words that does not exist and that doesn’t originate from the applied load, but that must be cinematically acknowledge (the frontier cinematic conditions must be met).

Within the Virtual Work principle there are two forms: virtual displacement principle and virtual force principle; the difference between these two is that in the first one it is considered the influence of real displacement on virtual forces while in the second the influence of the virtual forces is considered on the real displacements.

$$\int_v \delta \underline{\varepsilon}^T \underline{\sigma}\, dV = \int_v \delta \underline{u}^T \underline{p}\, d\,L \quad . \tag{18}$$

The equation (18), presented above represents a simplified example of the Virtual Work Principle when applied to a beam suffering only from axial displacements and forces. Here δ represents displacement or virtual deformation, $\delta\underline{\varepsilon}$ corresponds to the beam's extension, vector $\underline{\sigma}$ represents the normal tension on the transversal section of the beam and the displacement $(\delta\, \underline{u}^T)$ field and the distributed outer action ($\underline{p}$) represent the second component of the beam.

5.2 - Geometrical Model

In this chapter the model used throughout this work is shown in detail, its origin and all the changes it went through until the finalized form.

5.2.1 - Original Geometrical Model

In order to perform the FE analysis, a geometrical model closely resembling the real knee joint was necessary. Since the knee joint is an incredibly complex structure with several different components, each with very specific characteristics and morphologies, creating its 3D model from scratch is an incredibly challenging task in itself, therefore the geometrical model adopted for this initial study was obtained from the work performed by Diane Carvalho on her theses "Estudo biomecânico dos meniscos na articulação do joelho humano" [80] whom originally obtained it from the Open Knee project [81].

The Open Knee is a project aimed to providing a free open source access to a variety of three-dimensional finite element representations of the knee joint for predictive simulations of joint load and its effects on the structure; this platform allows anyone interested to use, test and edit the available models with eleven publications contributing to the development of this project, besides the studies performed by the Open Knee project development team, these studies can be accessed here [81].

The Open Knee project is, currently, still a work in progress funded by the National Institute of General Medical Sciences, National Institute of Biomedical Imaging and Bioengineering, National States License [81].

The model attained from the Open Knee project, and used originally by Diane, was created from a sample of the right knee of a female individual, age 70, weight 77.1 kg and height 1.68 m, cause of death cancer (pneumonia); the figure of the knee were obtained in the Cleveland Clinic Biomechanics Lab using a Magnetic Resonance (MR) scanner [81].

Throughout her work Diane modified and added several characteristics to the initial model from The Open Knee project. Therefore, and since Diane's finished model is the starting model for this work, it stands to reason to describe the more important aspects and changes done by her to the model.

Originally, the hole knee was modelled as a single component, hence the first task performed was to identify and divide the various parts of the knee, Diane separated the model into the following parts: the femur, tibia, femoral cartilage, tibial cartilage which in turn was

divided into its medial and lateral parts, the four major ligaments (ACL, PCL, MCL, LCL), and finally both the medial and lateral menisci [80].

Both the ligaments and meniscus had vertical bar elements introduced, for the ligaments these elements were an attempt to simulate the collagen fibres that constitute them and avoid the creation of false compression stress; while for the meniscus these elements served as a means to divide the meniscus into its two structural elements: the support matrix and the radial/circumferential collagen fibres. Two models of the medial meniscus were created, one with a vertical longitudinal lesion and another with a transversal lesion [80] but these were not used for this work.

Diane also defined the material properties for the various parts of the model, below there is a simplified table, table 1, with some of the values and characterizations used by Diane.

Table 5.1 – Material Properties of the starting model

Part	Matetial Characterization	Values
Tibia	Rigid Body	E = 14220 MPa; $\nu = 0.32$
Femur	Rigid Body	E = 14220 MPa; $\nu = 0.32$
Meniscus	Elastic Body	E = 59 MPa; $\nu = 0.45$
Cartilage	Elastic Body	E = 5 MPa; $\nu = 0.46$

As for the ligaments, these were characterized with the Neo-Hook model in which a group of properties were used for all the ligaments fibres and a different group of properties were used for the support matrix of the fibres.

For more detailed information please consult Diane's theses "Estudo biomecânico dos meniscos na articulação do joelho humano" [80].

5.2.2- Development of the Geometrical FE Model

As mentioned previously the model used for this study had to be modified from the model used by Diane.

The main modification was the introduction of the reinforcement to the ACL. Besides this the material characterization for the ligaments as well as the material property values used for most of the components needed to be updated and the stability of the model was, as a whole, needed to be improved, all of this will be further explained in a moment.

One of the minor changes that is still worth mentioning, is the smoothening of the general surface geometry of the model. This was achieved by increasing the number and diminishing the size of the model's elements, correcting the original model's sharper and cruder surface. This was done purely for aesthetic reasons, in order to get a more realistic looking model. Below we have the figure 20, with the original versus the current models.

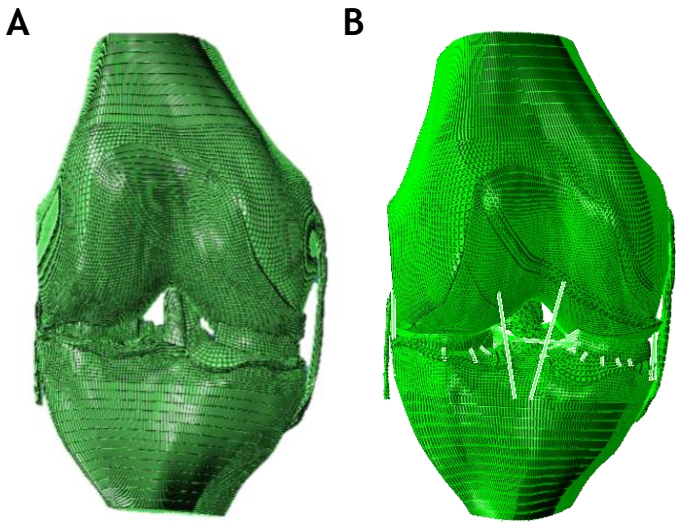

Figure 5.2 – [A] Original Model surface geometry; [B] Model surface Geometry post smoothening

5.2.3- Creating the ACL-Reinforcement Component

The ACL from the original model had to be replaced since it was not originally made to have a reinforcement within it. Therefore, the ACl was removed from the original model and had to be remade.

The program used for this was SolidWorks, which is a solid modelling computer-aided design software program.

The process for rebuilding the ligament was as follows, first the whole knee model was exported from Abaqus and imported to Solidworks as an STL file format, see figure 21 [A], then the ACL was isolated, see figure 21 [B].

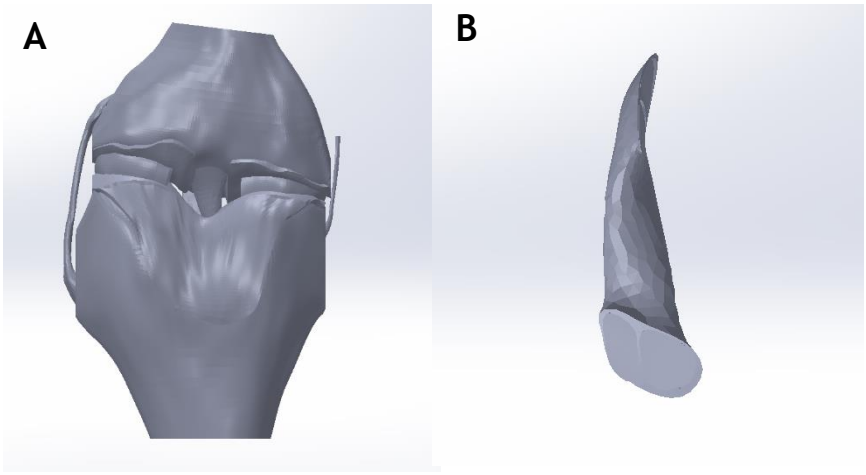

Figure 5.3 – [A] Entire Knee Model in SolidWorks; [B] Isolated ACL in SolidWorks

The next step was to outline the surface of the ACL in order to create a new solid that would be as similar as possible to the original ACL.

To do this, 35 new planes were created at fixed distances from each other. In each plane a 2D sketch of the surface of the ligament was drawn, these sketches would then serve as a guideline to the creation of the new solid through the “Lofted Boss/Base” command which adds material between profiles/sketches, figure 22.

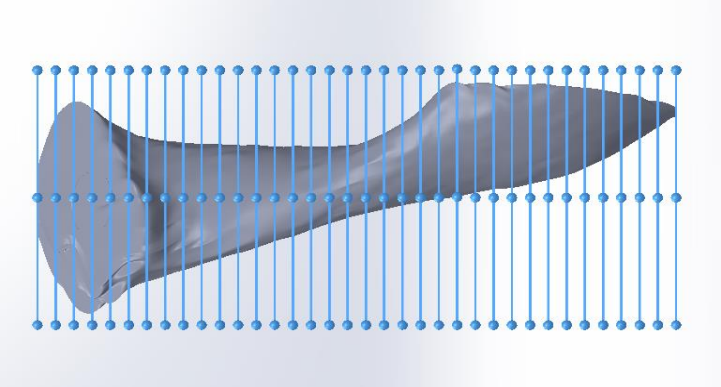

Figure 5.4 – Solid created from the original ACL

With the base solid ACL created a cylindrical cut passing through the entire length of the ligament was created, this would be the place in which the reinforcement part would be located. To do this the same technique was used as previously but this time the profiles drawn were of circles which would serve as the guideline for the “Lofted Cut” command, which removes material between profiles/Sketches, figure 23.

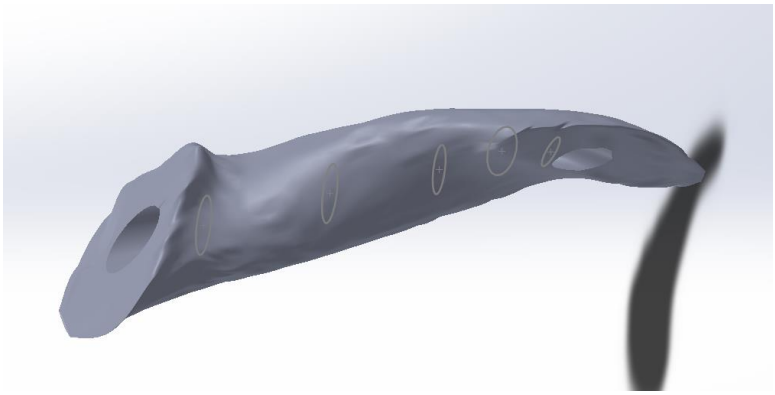

Figure 5.5 – New solid ACL with the profile for the Reinforcement cut

Finally, the space left by the cut was filled, creating the part which would become the reinforcement. For this the same profiles used for the cut were used in conjunction with the “Lofted Boss/Base” command, figure 24.

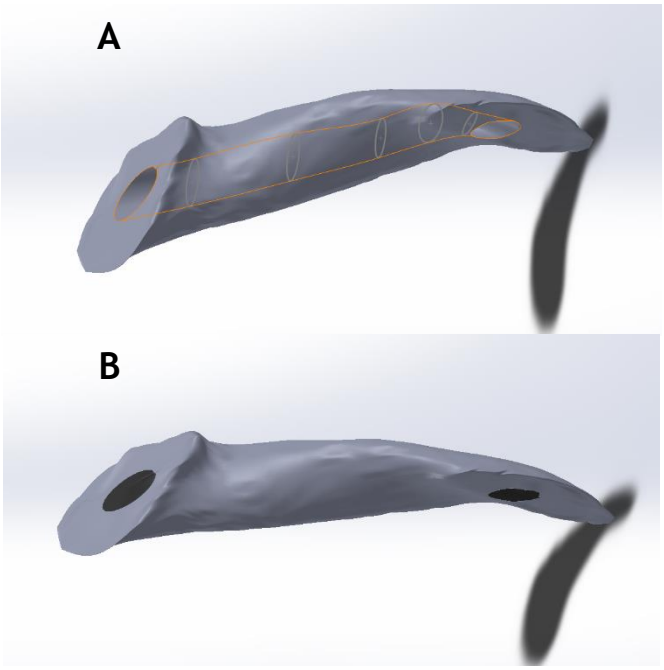

Figure 5.6 – [A] New ACL solid prior to the filling of the cut area; [B] New ACL with the Reinforcement

With the new ACL created, the model was exported back into Abaqus as an .igs file. In Abaqus the model was imported as two separate parts one being the "Ligament" and the other being the "Reinforcement".

The procedure now was to prepare the ACL-Reinforcement to be integrated into the knee model.

In here a first characterization of the material properties and fibre orientation of both the Ligament and Reinforcement was done.

The next step was the assembly of the two parts, in this step both would be tied to each other by a master/slave constraint, making it so they would not pass through each other when in movement.

As for the mesh creation, the element type was different for the ligament and reinforcement. The mesh created for the ligament consists of 10-node tetrahedron hybrid with linear pressure elements (C3D10H) while the mesh created for the reinforcement consists of 8-node linear brick hybrid with constant pressure (C3D8H), se figure 25.

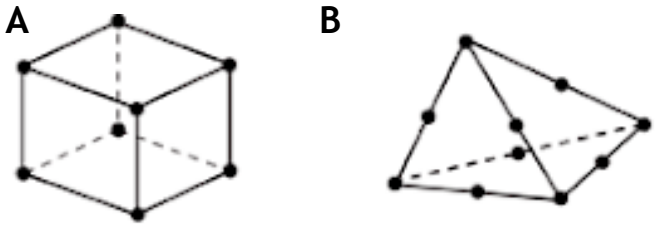

Figure 5.7 – [A] Linear element (8-node brick, C3D8); [B] Modified Second-order element (10-node tetrahedron, C3D10); modified from [82]

Once the new ligament was properly meshed it was exported has an input file to be introduced to the knee model.

5.2.4- The input files

The input files in Abaqus are text files composed by an intuitive keyword-based format that contain a complete description of the model in question. These files are easily modifiable allowing for a higher degree of model customization and the tests performed on it. Making these the primary tool used throughout this work.

Before advancing, an explanation of the structure of this model and its input (inp) files is in order.

This model possesses over 100 inp files. The “Main” inp is the file in which the information from all the other inp files is gathered, it’s also in this one that the test and analysis parameters are defined.

In the “Main” inp, other eight inp files are called. These being: the Nodes inp file, Structure inp file, Materials inp file, Ties inp file, Surfaces inp file, Contact inp file, and the final three can be summed up as Spring inp files.

5.2.5- Nodes and Structure input files

The Nodes and Structure inp are similar in nature, the first contains all the nodes that comprise the model while the second contains the elements that represent each part of the model.

The entire model, figure 26, is composed by 103465 nodes in total.

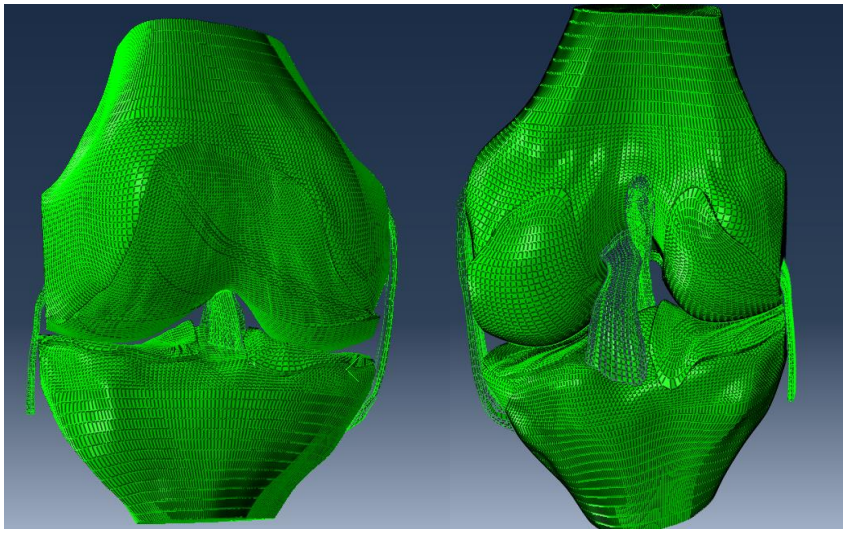

Figure 5.8 – Anterior and Posterior view of the whole model

These nodes comprise the elements the make up every part of the model.

Starting with the bony parts, the femur is composed by 13862 nodes and 13859 elements and the tibia is composed by 11361 nodes and 11359 elements, see table 2 below

Table 5.2 – Nodes and Elements that make up the Femur and Tibia in the final model

Part	Nodes	Elements	Element Type
Femur	1 - 13862	56434 - 70293	S4
Tibia	13863 - 25224	70294 - 81653	S4

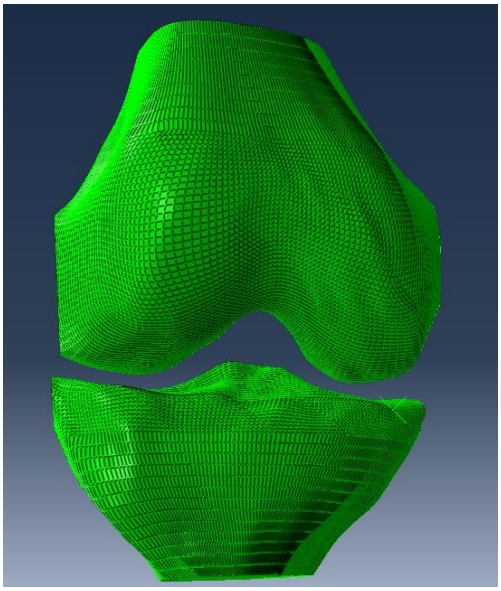

Figure 5.9 – Mesh representing the Femur (top) and Tibia (bottom) parts

Now for the cartilaginous parts there is the Femoral Cartilage which has 23799 nodes and 17226 elements, the left Tibial Cartilage which has 6527 nodes and 4715 elements and the right Tibial Cartilage which has 5727 nodes and 4130 elements, see table 3 below.

Table 5.3 – Nodes and Elements that make up the Femoral and Tibial Cartilage in the final model

Part	Nodes	Elements	Element Type
Femoral Cartilage	25225 - 49024	1 - 17226	C3D8H
Tibial Cartilage (Left)	49025 - 55552	17227 - 21942	C3D8H
Tibial Cartilage (Right)	5555 - 61280	21943 - 26073	C3D8H

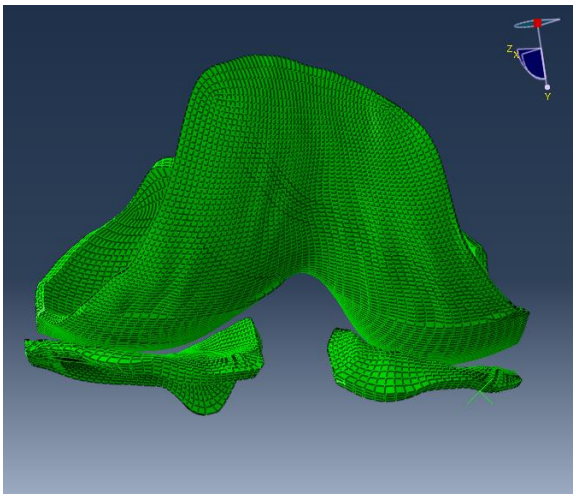

Figure 5.10 – Mesh representing the Femoral (top) and Tibial (bottom) Cartilage

As for the meniscus, the Medial Meniscus is composed by 5894 nodes and 4549 elements and the Lateral Meniscus is composed by 5895 nodes and 4549 elements, see table 4 below.

Table 5.4 – Nodes and Elements that make up the Medial and Lateral Menisci in the final model

Part	Nodes	Elements	Element Type
Medial Meniscus	80383 - 86277	42470 - 47019	C3D8H
Lateral Meniscus	74487 - 82382	37850 - 42399	C3D8H

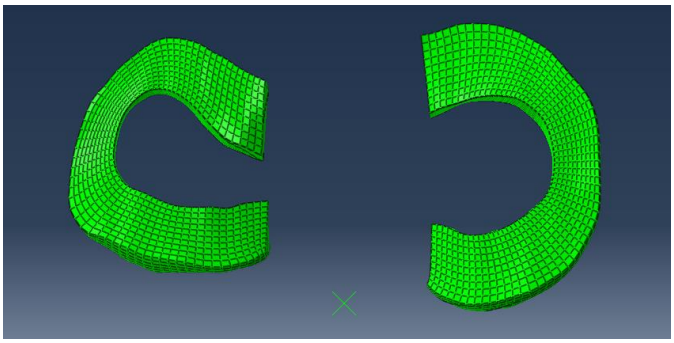

Figure 5.11 – Mesh representing the Medial (right) and Lateral (left) Menisci

Finally, for the four major knee ligaments and reinforcement, the LCL is composed by 7424 nodes and 6655 elements, the MCL is composed by 5780 nodes and 5119 elements, the PCL is composed by 5921 nodes and 5247 elements, the ACL is composed by 5981 nodes and 3221 and the Reinforcement is composed by 629 nodes and 439 elements. See table 5 below:

Table 5.5 – Nodes and Elements that make up the Four Major Ligaments and the Reinforcement in the final model

Part	Nodes	Elements	Element Type
LCL	67062 - 74486	31194 - 37849	C3D8H
MCL	61281 - 67061	26074 - 31193	C3D8H
PCL	86279 - 92200	47090 - 52337	C3D8H
ACL	96854 - 102835	81654 - 84875	C3D8H
Reinforcement	102836 - 103465	84876 - 85315	C3D10H

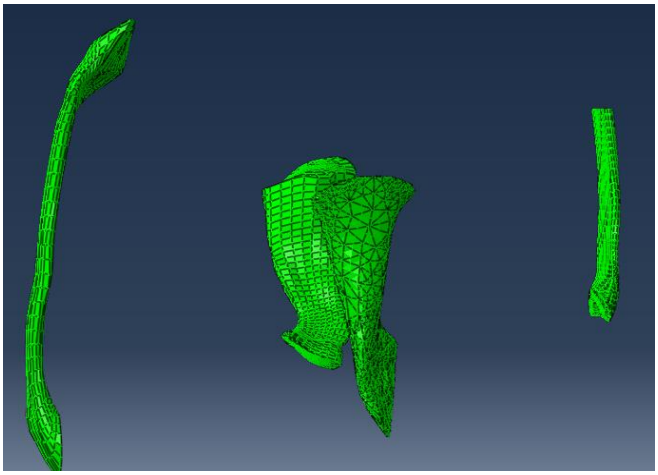

Figure 5.12 – Mesh representing the Four Major Ligaments in the Final Model

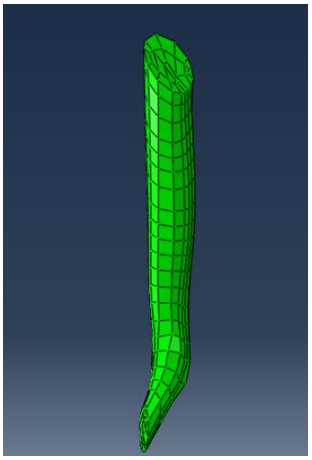

Figure 5.13 – Mesh representing the Reinforcement in the Final Model

5.2.6- Materials input files

In the Materials inp file is where all the parts of the model have their material properties established.

The material property values for the all the elements of the knee joint were obtained through an analysis of the information in the "FEM Analysis of the Human Knee Joint: A Review" [24], this is a document in which a large number of data from various studies in the FEA of the human knee joint are gathered. The characterization of the ligaments was changed from the original in order to be more accurate and up to date with literature.

One very important point to get across is that in the material properties given here for the reinforcement, doe to the lack of existing literature on its material parameters, were obtained through the use of Online Materials Information Resource (MatWeb) [83] and the simplified HGO equations, that will be explained below.

Following the same order as previously: the bones are classified as rigid bodies; the meniscus and cartilage were classified with an elastic behaviour and both the ligaments and the reinforcement are classified with an Holzapfel-Gasser-Ogden (HGO) hyperelastic behaviour. In table 6 below are presented the material definitions and values used.

Table 5.6 – Material Properties of all the components of the final Knee Model

Part	Material Characterization	Values	Source
Tibia	Rigid Body	-	[84, 85, 86]
Femur	Rigid Body	-	[84, 85, 86]
Meniscus	Elastic	E = 120 MPa; ν = 0.45	[87, 88]
Cartilage	Elastic	E = 15 MPa; ν = 0.475	[89, 90]
LCL	Anisotropic Hyperelastic (HGO)	C10= 1.0; D= 0; K1= 41.21; K2= 5.26; K3= 0.0	[87, 91, 92]
MCL	Anisotropic Hyperelastic (HGO)	C10= 1.0 MPa; D= 0; K1= 28.01 MPa; K2= 1.07; K3= 0.0	[87, 91, 92]
PCL	Anisotropic Hyperelastic (HGO)	C10= 1.0 MPa; D= 0; K1= 46.42 MPa; K2= 2.73; K3= 0.0	[87, 91, 92]
ACL	Anisotropic Hyperelastic (HGO)	C10= 1.0 MPa; D= 0; K1= 52.52 MPa; K2= 5.86; K3= 0.0	[87, 91, 92]
Reinforcement	Anisotropic Hyperelastic (HGO)	C10= 0.685 MPa; D= 0; K1= 30.0 MPa; K2= 8.0; K3= 0.0	-

As mentioned previously, and seen in table 5, when compared to the set of material properties used on the original model, the values used for the material properties of all the components was changed as well as the material characterization for the ligaments, which was changed to the HGO model.

The HGO constitutive model was first developed by Gasser et al. [93] with the objective of creating a reliable model that was capable of accurately describing the nonlinear elastic behaviour of arterial tissue. With their continuous work Gasser et al. achieved a model especially suited to describe the anisotropic hyperelastic behaviour of collagen fibre reinforced tissue by adding a scalar parameter that accounts for the dispersion of collagen fibres [94,95].

Even though this model was developed for arterial tissue, it has already been applied to represent different soft tissue like knee ligaments [14,96] successfully and with better results than previous methodologies, making it a perfect fit for this work.

In order to better understand the HGO model some concepts will be now presented, for more detailed and technical information the reader is referred to the original article [93] and to the Abaqus theory Manual [97].

Before diving into the HGO specific concepts some more general concepts are presented first. Consider equation 19 below, which represents deformation gradient.

$$F(X) = \frac{\partial \mathrm{x}}{\partial \mathrm{X}} \quad . \tag{19}$$

The deformation gradient (F), describes the local kinematics of deformation in which X is the position of a material point in the reference conFiguretion and x represents the material point in the deformed conFiguretion.

The Jacobian (J) basically refers to the ratio of the reference volume over the deformed value, only for a homogeneous deformation on a material.

$$J = det\ F = \frac{\rho_0}{\rho} \quad , \tag{20}$$

where ρ_0 represents the reference density and ρ represents the deformed density.

The Cauchy-Green deformation tensors (C and B) form the basis for constitutive hyperelastic model development applied to soft tissues, it provides information on the deformation measures independent of rigid body rotations.

$$F = F^T F \ and \ B = FF^T \quad . \tag{21}$$

The Strain Energy Density Function is a function that defines the deformation at a given point as:

$$\Psi = \Psi\ (F) \quad . \tag{22}$$

If the material is isotropic, equation 22 become:

$$\Psi = \Psi\ (I_1, I_2, I_3) \quad , \tag{23}$$

in which,

$$I_1 = tr(C) = \lambda_1^2 + \lambda_2^2 + \lambda_3^2 \ ; \ I_2 = \frac{1}{2}[(tr(C))^2 - tr(C^2)] \ ; I_3 = det\ C. \tag{24}$$

Starting now with HGO concepts. The deformation gradient can be composed by a volumetric part ($J^{1/3}I$), that accounts for deformations that change the volume, and an isochoric part $\overline{F}$, which with its volume conserving nature means that det $\overline{F}$ = 1 constantly.

$$F = (J^{1/3}I) * \overline{F} \quad , \tag{25}$$

in which I represents the identity and J representing the Jacobian of the transformation.

In consideration of eq. 25 the Cauchy-Green deformation tensor becomes:

$$\overline{C} = \overline{F}^{T}\,\overline{F} = (J^{-2/3}C) \tag{26}$$

Now, with a material composed by two different families of fibres, each of the families will be characterized by a mean referential direction around which these fibres are distributed with rotational symmetry. In this reference direction there are two distinct directions which are defined by two-unit vectors $\boldsymbol{a}0i$, i = 4,6. Defining two more invariants:

$$I_4 = a_4 * (Ca_4), \qquad I_6 = a_6 * (Ca_6) \quad . \tag{27}$$

With these the isochoric counterparts of I_1, I_4 and I_6 become:

$$\overline{I_1} = tr(\overline{C}) = J^{-2/3}I_1, \ \overline{I_4} = J^{-2/3}I_4, \ \overline{I_6} = J^{-2/3}I_6 \quad . \tag{28}$$

Now it is possible to define the Strain Energy Density Function of the HGO model, this is divided into three parts: volumetric, isotropic and anisotropic.

$$\Psi\,(C, a_{04}, a_{06}) = \Psi_{vol}\,(J) + \overline{\Psi_{iso}}(\overline{C}) + \overline{\Psi_{aniso}}(\overline{C}, a_{04}, a_{06}) \quad . \tag{29}$$

Since the original model did not include a volumetric term it was necessary for Abaqus to introduce it as a penalty function that accounts for compressible behaviour.

$$\Psi_{vol}(J) = \frac{1}{D}\left(\frac{(J^{el})^2-1}{2} - ln\,J^{el}\right) \quad , \tag{30}$$

where J^{el} represents the elastic volume and D is related to the bulk modulus (K_0) by D= $2/k_0$.

If D=0 the model is considered incompressible.

As for the isotropic component of the model, it serves to model non-collagenous ground matrix where it uses the neo-Hookean parameter C10.

$$\overline{\Psi_{iso}}(\overline{C}) = C10(\overline{I_1} - 3) \tag{31}$$

Lastly, the anisotropic component accounts for the two fibre families with different directions in the ground matrix. This component is defined as:

$$\overline{\Psi_{aniso}}(\overline{C}, a_{04}, a_{06}) = \frac{K_1}{2K_2}\sum_{i=4,6}\left\{exp\left[K_2\left(\overline{E_i}\right)^2\right] - 1\right\} \quad , \tag{32}$$

With,

$$\overline{E_i} \stackrel{\text{def}}{=} k(\overline{I_1} - 3) + (1 - 3k)\left(\overline{I_i} - 1\right) \quad . \tag{33}$$

The parameters C10, D, K_1 and K_2 are responsible for characterizing the stress-strain responses that the material will have.

The parameter k derives from the statistical distribution function which governs the fibres orientation and distribution in the reference conFiguretion. K can only possess values between 0 and 1/3, with 0 meaning that the fibres are perfectly aligned with each other and 1/3 meaning that the fibres are completely randomly distributed, see image 32 below for a visual representation of this.

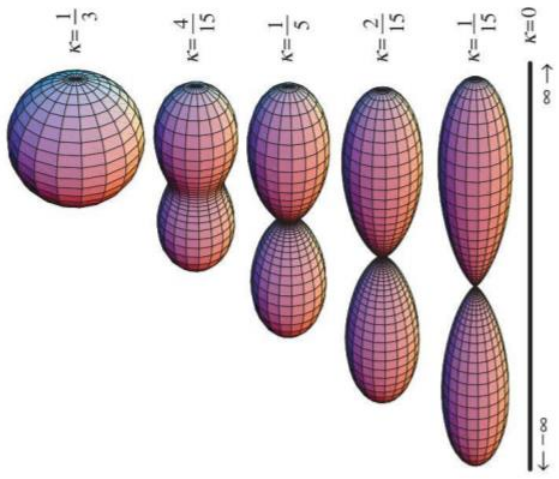

Figure 5.14 – Representation of the effect of k values on the statistical equation [94]

5.2.7- Surface, Ties and Contact input files

With the material properties of the model in place, the next step is to make sure that the model's various components stay in their positions during testing and movement and this is done through the Surface inp, the Ties inp and the Contacts inp.

Starting with the Surfaces inp file, within this file is where surfaces of all the parts that are in contact with others are highlighted. For example, one of the ACL's ends contacts with the femur; so in order to create contact between these, the elements at the top of the ACL

and some elements of the femur will each be highlighted, see figure 33 below, through a SURFACE command that will then be used to create the pairings in the ties inp.

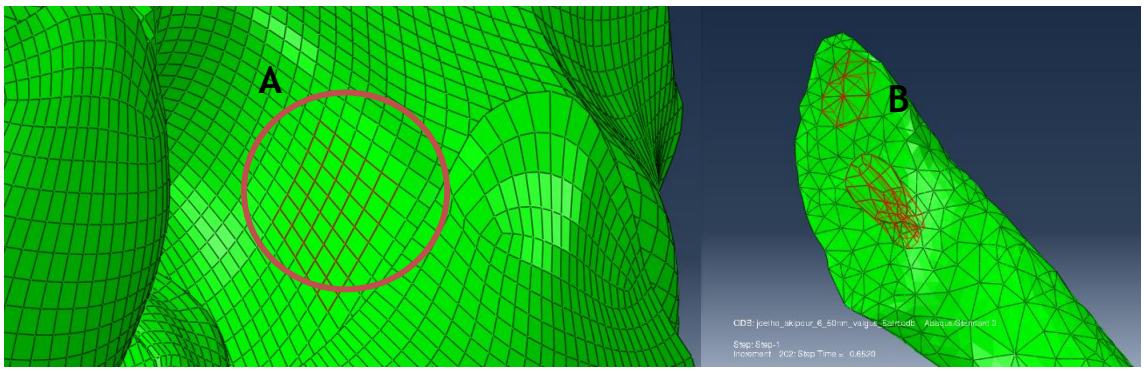

Figure 5.15 – [A] Highlighted Femur elements for contact tie; [B] Highlighted some Ligament and Reinforcement Elements for contact tie.

With all the contact surfaces created it is possible then to define the interacting pairs in the ties and contacts inp files.

The Ties inp file, as the name sugests, is a file based on the Tie function command. This command makes it so two sets of elements in different meshes be bound to eachother with one being the "master" surface and the other the "slave" surface, this basically makes it so the slave surface can not penetrate the master surface while the other way around can happen. The criteria to choose the master and slave surface are as follows: the master surface should be the larger surface, if the size is similar the stiffer surface should be the master, if the size and stifness are similar the master surface should be the one with coarser mesh.

With these points in mind the selection of interacting pairs was as follows: (Slave-Master)

- Femur surface – MCL surface
- Tibia surface – MCL surface
- Femur surface – LCL surface
- Femur surface – PCL surface
- Tibia surface – PCL surface
- Left Tibial Cartilage surface – Tibia surface
- Right Tibial Cartilage surface – Tibia surface
- ACL surface – Femur surface
- Reinforcement Surface - Femur surface
- ACL surface – Tibia surface
- Reinforcement surface – Tibia Surface

Now onto the Contact inp file, this file is responsible to establish CONTACT PAIR interactions. This type of interaction defines what surface may contact and interact with each other during analysis, this command was mainly appiled to the meniscus and cartilage parts of the model:

- Lateral Meniscus surface – Femoral Cartilage surface
- Medial Meniscus surface – Femoral Cartilage surface
- Medial Meniscus surface – Right Tibial Cartilage surface
- Lateral Meniscus surface – Left Tibial Cartilage surface
- Left Tibial Cartilage surface – Femoral Cartilage surface
- Right Tibial Cartilage surface – Femoral Cartilage surface

One major problem that the original model had was stability, making it so when running a simulation in any kind of test, there was the possibility of the test not completing due to this. This instability would manifest more prominently in the meniscus. Depending on the test, these would exhibit excessive and unnatural movement and would penetrate through the surface of the parts it was in contact with.

To solve this problem various truss elements were introduced to the model, see figure 34, these would allow the meniscus to move within a certain range of motion determined by the properties given to the element and would guaranty that penetration would be less likely to happen.

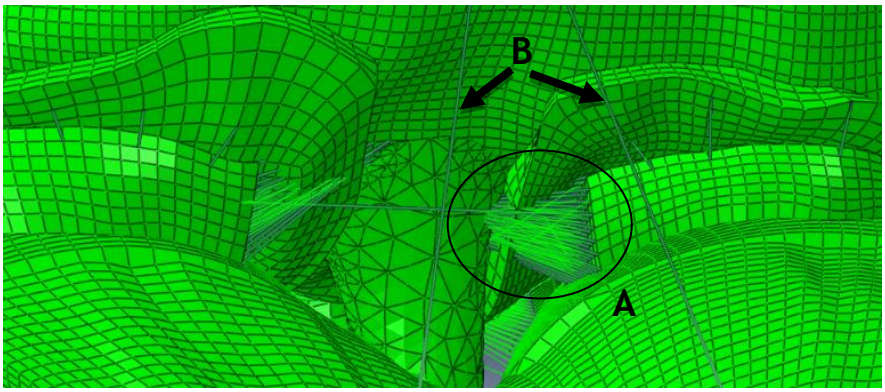

Figure 5.16 – [A] Meniscus Truss elements; [B] Truss elements added for general stability of the model.

Chapter 6

Results and Discussion

To simulate the movement of the knee with the objective of verifying the efficacy of the reinforcement, the tests were performed based on a case that has been tested experimentally [23] and through FE studies [21,23,37] in literature.

This case entails the application of a force of 134N, anteriorly, on the Tibia at certain flexion angles. It was designed to simulate the Lachman anterior drawer test, which is used to diagnose the ACL deficiency.

During this work the force was applied in the Femur and the Tibia was fixed in all degrees of freedom, see figure 35, while normally this is done the other way around this does not make a considerable difference since the posterior displacement of the femur with the Tibia fixed would be equal to that of the anterior displacement of the Tibia with the Femur fixed.

In order to be able to test efficacy of the reinforcement, in a first step the rotation of the Femur was applied, this rotation was bound to node 2749 at the top of the femur. In a second step the force of 134N, directed posteriorly, was placed on the same point. This guaranteed that the force applied would always be on the anterior-posterior axis, simulating the normal displacement of this structure during movement.

The force was applied at the angles of rotation 0, 15 and 30 degrees of flexion, the data obtained was about the kinematic behaviour of the model with focus on the ACL-reinforcement component. The values for maximum principal stress for the hole model and for the ACL-Reinforcement components are obtained and compared with existing values in the literature; for the second and third case additional data on the contact pressure values are obtained for the menisci and cartilaginous components.

The data used for comparison are: the study performed by David Fernandes on his theses “Finite Element Analysis of the ACL-deficient Knee” in which he used a similar FE approach to simulate an healthy and deficient knee model [89], the studies performed by Pena et al [21,37] and Song et al [23].

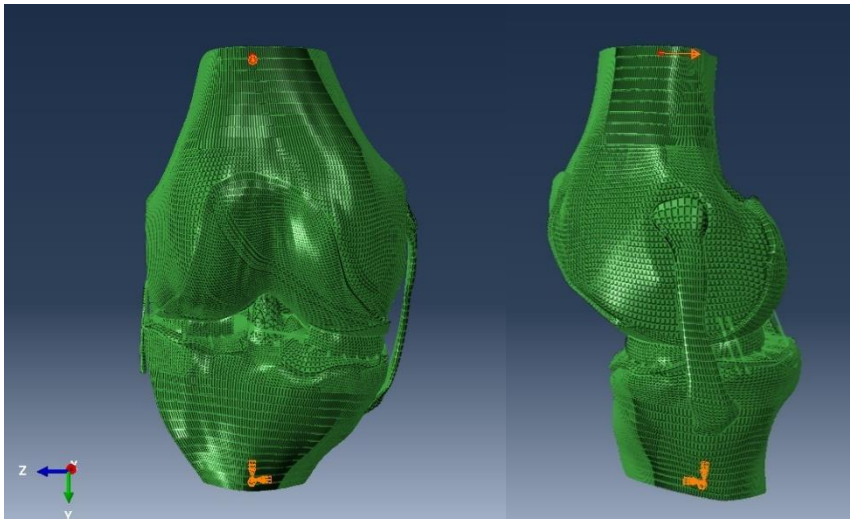

Figure 6.1 – Frontal and Side view of the Final Model

6.1- Case 1 (0° of Rotation)

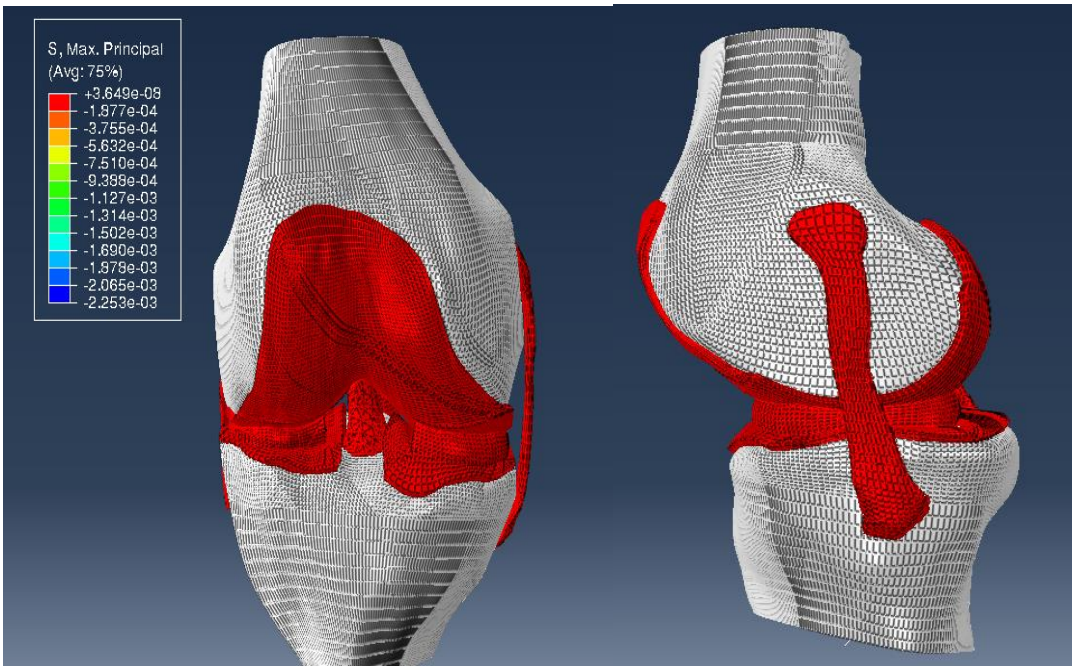

Figure 6.2 – Case 1, Anterior and Lateral view of the Knee joint model after the application of a posterior 134N force to the Femur.

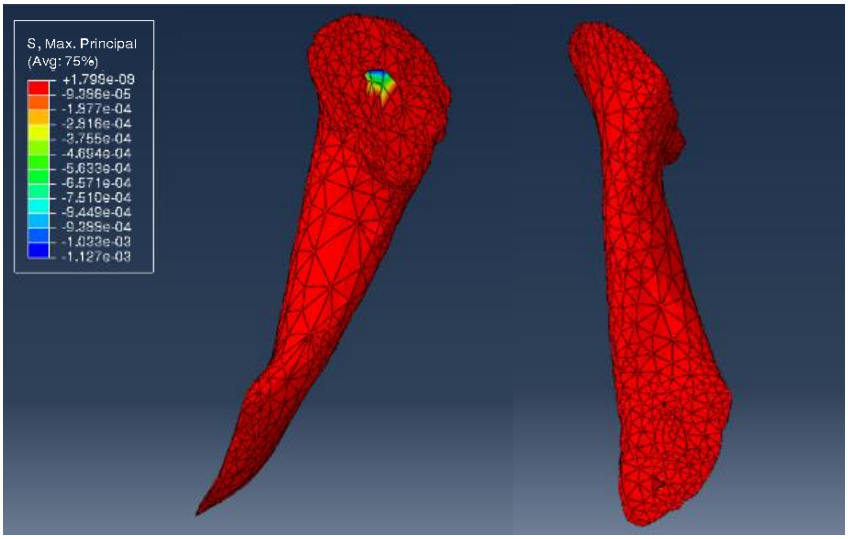

Figure 6.3 – Case 1, view of the ACL-Reinforcement's Tibial and Femoral insertion after the application of the posterior 134N force to the Femur.

Figure 36, above, represents the maximum principal stress (max. principal stress) results obtained from the test of the knee model when under a 134N posterior femoral force when in full extension (rotation of 0°). In this figure we can ascertain that the whole joint is under really low max. principal stress values, this is what was expected since in this position the components of the knee joint are mostly unaffected.

One important thing to note is that normally the ligaments of the knee even in full extension are in a state of stress, these are called residual stresses, this however was not possible to include in the model because in Abaqus it is not possible to set pre-stress to anisotropic hyperelastic models. But Limbert et al. [12] performed a study in which he compared a stress free and pre-stressed ACL and he what found was that the in both cases the stress distributions were similar, and the only difference was being that in the pre-stressed ACL the magnitude of the values was higher.

Looking now at figure 37 the first statement can be further confirmed, the ACl-Reinforcement component present low values of max. principal stress. Again, since the model is in full extension this is expected and corroborates with the fact that this is the component that restrains force of anterior translation.

6.2- Case 2 (15° of Rotation)

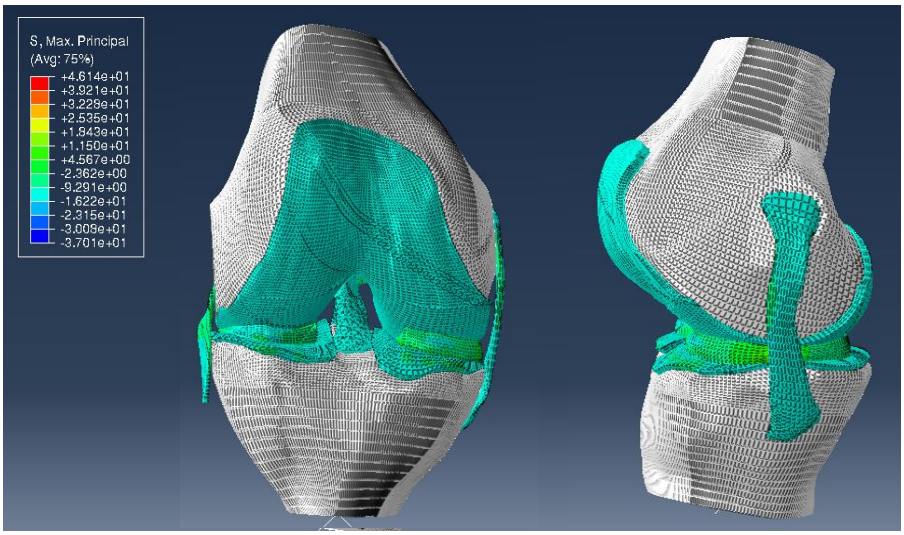

Figure 6.4 – Case 2, Anterior and Lateral view of the Knee joint model after the application of a posterior 134N force to the Femur.

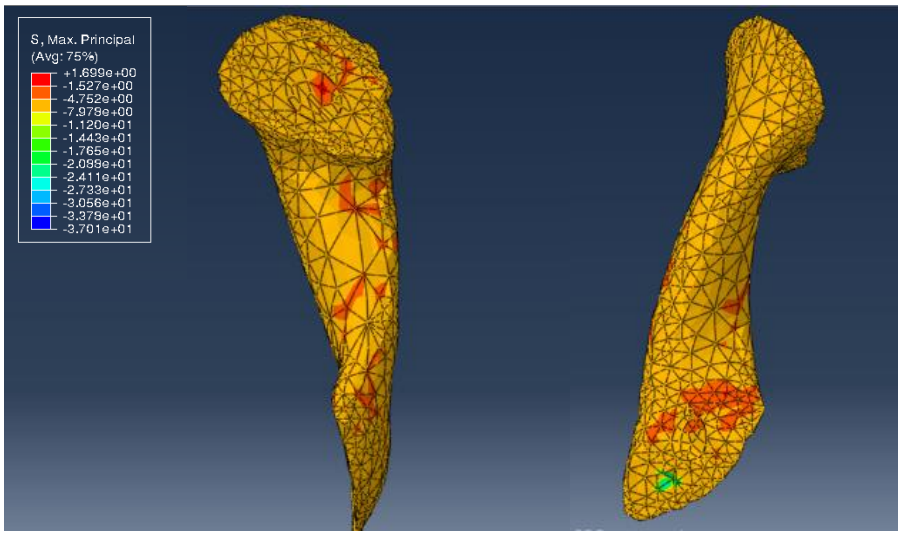

Figure 6.5 – Case 2, view of the ACL-Reinforcement's Tibial and Femoral insertion after the application of the posterior 134N force to the Femur.

Figure 38 shows the results of the tests performed on the knee model when under 134N of posterior force applied on the Femur at 15° of rotation.

Comparatively to the first case, at full extension, here we start to see max. stress values on the model. The results present a max stress value of 46 MPa which is comparable to the results found in [98].

But, now looking at figure 39, which represents the ACL-Reinforcement component, the results show that this component is under some stress, but the values are not as high as what was expected.

The experimental data obtained by Pena [21] shows that, a healthy ACL under full extension conditions should have an average max. principal stress of 6.5 MPa and a maximum value of 15 MPa, another similar study by Song et al [23] puts the average at 6.9 MPa and maximum at 24 MPa. Comparatively, the values here presented are considerably lower than those specially when considering that in this case there is rotation applied to the model.

This may be a reason to believe that the Reinforcement, with the material values given here, is not providing enough support to the structure. To confirm this hypothesis, and since the overall max. principal stress of the model corresponds to what is expected, the other components were checked.

For the other four major ligaments, the LCL/MCL/PCL, the stress values obtained were somewhat higher than the data found by David in his work [91] but close to the values found by Kanamori et al [90], specifically for the MCL. The values not being significantly different, it was considered that these components were not affecting in any major way the results obtained above.

The next components to be checked would be the meniscus and the cartilaginous parts, and here is where more interesting and conclusive results appeared.

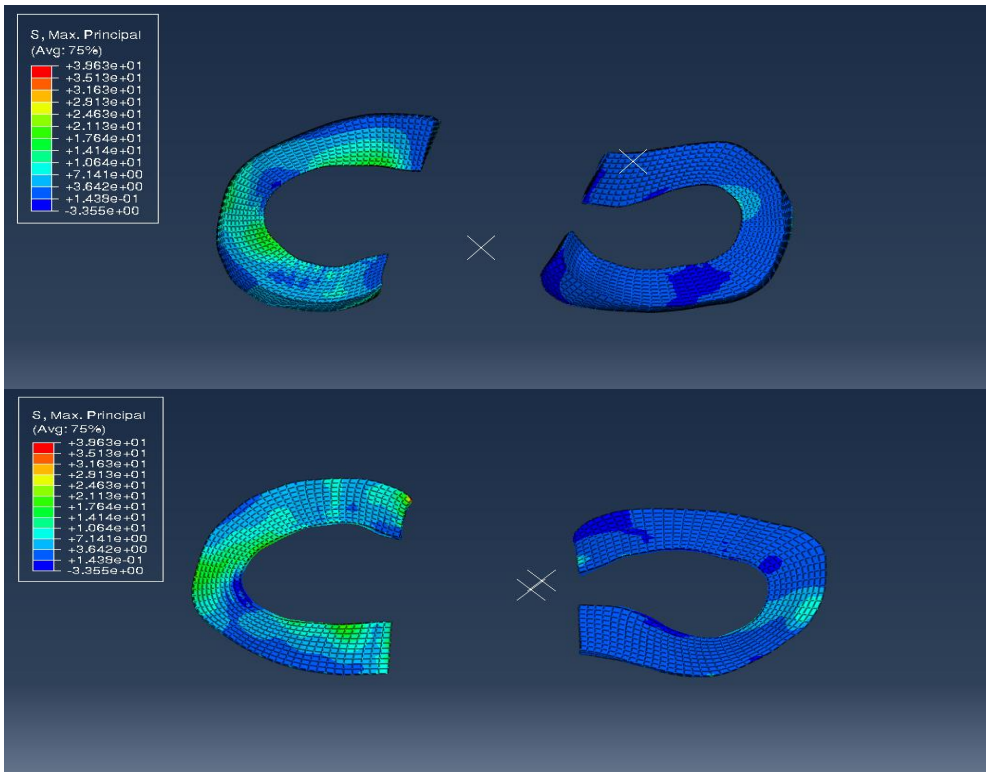

Figure 6.6 – Case 2, Max. Principal Stress on the Medial and Lateral Meniscus, superior and inferior view.

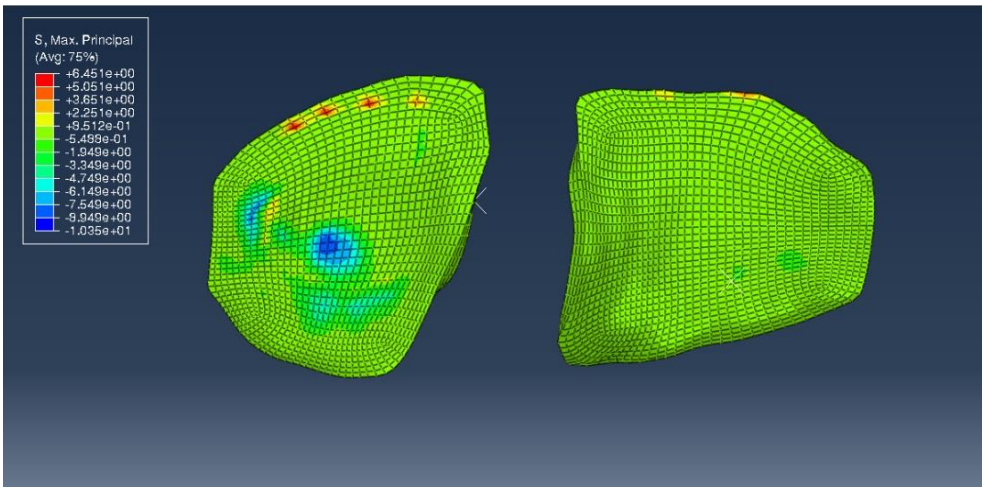

Figure 6.7 – Case 2, Max. Principal Stress on the Left and Right Tibial Cartilage

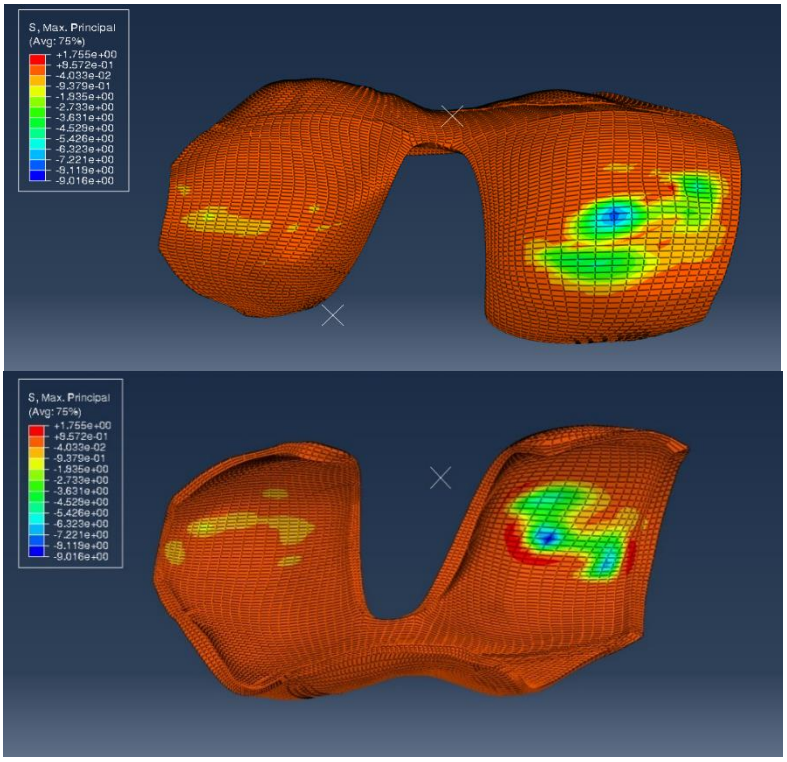

Figure 6.8 – Case 2, Max. Principal Stress on the Femoral Cartilage

In Figure 40 to 42, above, the max. principal stress results for the Menisci and Cartilaginous components at the rotation of 15˚ are shown.

Following the previous line of thought, the stress values on the meniscus were examined. As it is possible to see in figure 40 the max principal stress values reach values of 38.6 MPa with the average value being close to 10 MPa, higher stress values manifest more heavily on the Medial Meniscus which is expected since this is the meniscus that usually starts contact with the cartilage first.

These values are a lot higher when compared to the work of Dennis John et. al. [100] and the values obtained by Diane [80], in figure 43 below there is an example of the values expected for the menisci when in similar conditions.

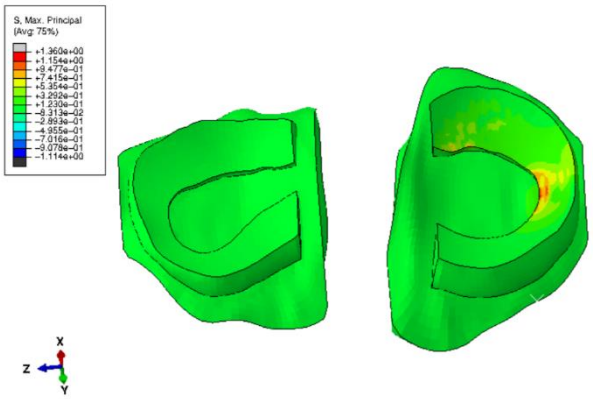

Figure 6.9 – Case 2, Max. Principal Stress results for the menisci at a rotation angle of 15 °, Values obtained by Diane [80]

In the example in Figure 43 the highest stress value is 1.36 MPa, which aligns with the results obtained by Dennis John et. al., comparatively this value is only a third of the highest value on the results presented in Figure 40. This leads to the conclusion that the menisci components of this model are under higher general stress values than they are supposed to under same conditions.

The same applies to the Femoral and Tibial Cartilage when looking at figure 41 and 42, both present high values of max. principal stress, more specifically on the zones that are in direct contact with the meniscus, which stands to reason, with the more prominent area being the one in contact with the medial meniscus.

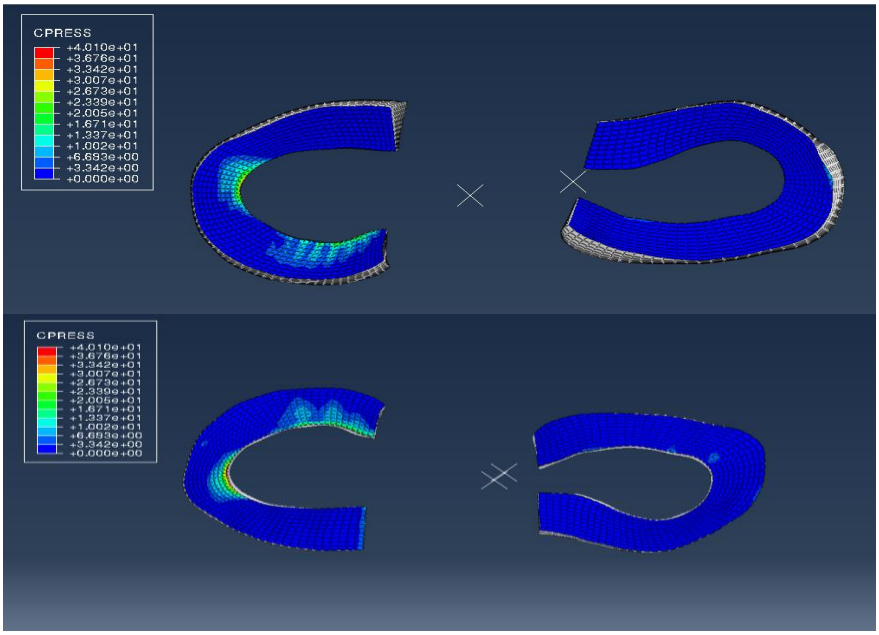

Figure 6.10 – Case 2, Contact Pressure on the Lateral and Mediual Meniscus, superior and inferior view

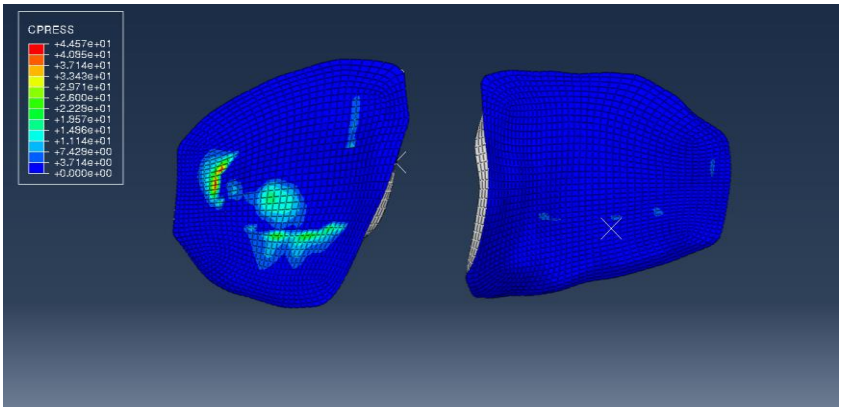

Figure 6.11 – Case 2, Contact Pressure on the Left and Right Tibial Cartilage

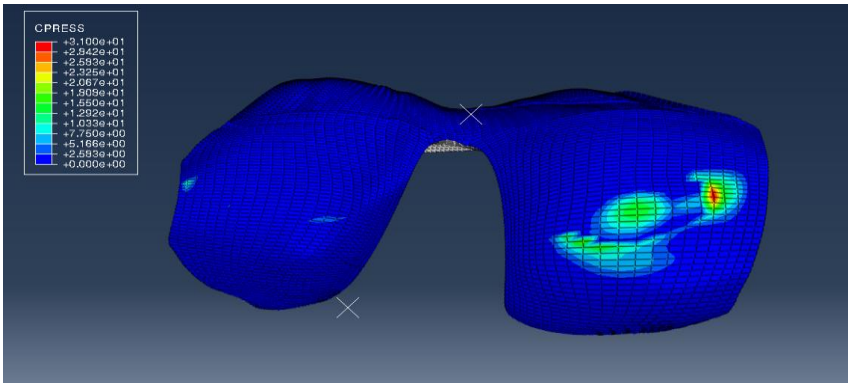

Figure 6.12 – Case 2, Contact Pressure on the Femoral Cartilage

For further confirmation the contact pressure data for the Menisci and Cartilage components was taken and is shown in the figure 44 to 46 above.

From figure 43 we see the contact pressure values for the menisci, the interesting aspect here is that not only the values are higher than expected but the pressure distribution is as well. The highest contact pressure value is close to 40 MPa though these higher values seem to only exist on a relatively small region, on the interior of the Medial meniscus, with the majority of the component under values between 0.33 MPa to 20 MPa. Either way these values are extremely higher than the ones obtained by Diane [80], with her values not even reaching 5MPa see figure 47 below.

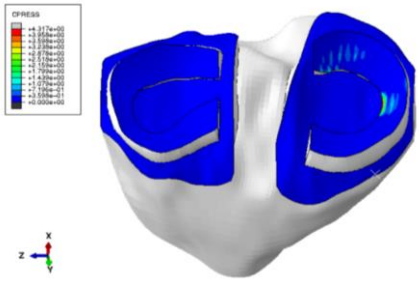

Figure 6.13 – Contact Pressure results for the Menisci at a rotation angle of 15°, Values obtained by Diane [80]

Again, the meniscus more affected at this rotation angle is mostly the Medial meniscus, therefore the higher values are located on it, and normally the area affected by the highest values should not be has large has it is shown in figure 44.

Once more, looking at figure 45 and 46, in both Femoral and Tibial Cartilage the contact pressure results are higher than expected. These values are only noticeable on the area that is in contact with the Medial meniscus, not being noticeable on the other side that contacts with the Lateral meniscus.

6.3 - Case 3 (30˚ of Rotation)

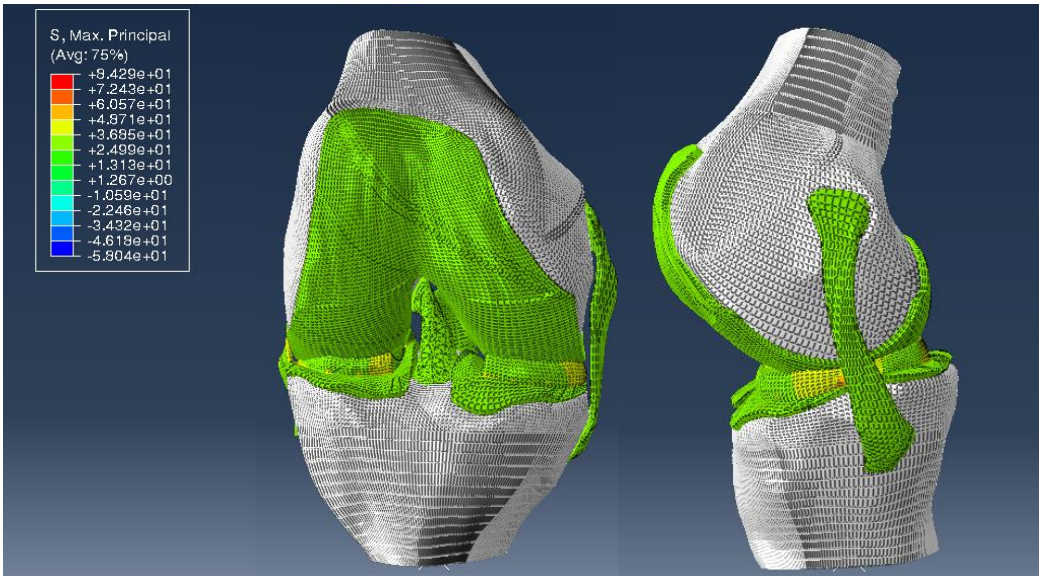

Figure 6.14 – Case 3, Anterior and Lateral view of the Knee joint model after the application of a posterior 134N force to the Femur.

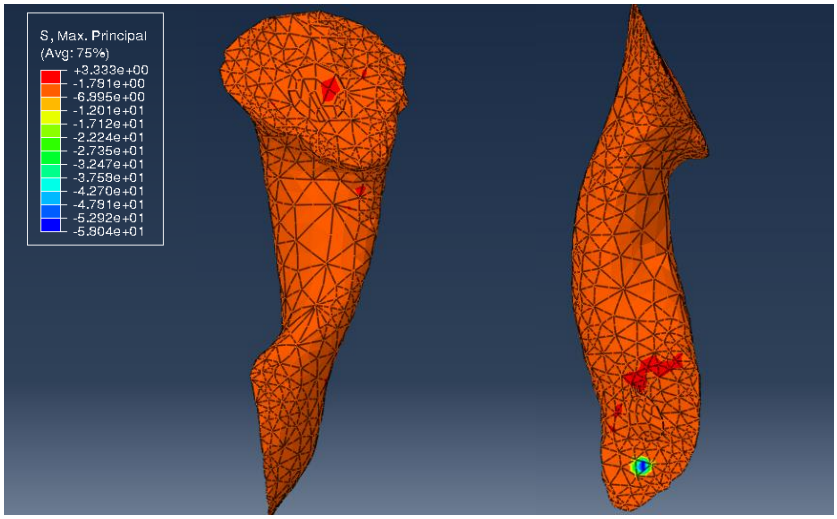

Figure 6.15 – Case 3, view of the ACL-Reinforcement's Tibial and Femoral insertion after the application of the posterior 134N force to the Femur

Figure 48 shows the results of the tests performed on the knee model when under 134N of posterior force applied on the Femur at 30˚ of rotation.

In this figure it is possible to see higher max. principal stress values than in the previous case, with 15˚ of rotation, this supports the fact that at higher degrees of flexion the function of the total structure becomes more demanding and the work load increases in order to prevent excessive anterior-posterior movement. Once again, the values shown in figure 46 are within what was expected with a maximum value of around 94 MPa, which is somewhat higher than the 84MPa obtained by David [98] but the general value distribution is still within reason.

Figure 49 looks more specifically at the ACL-Reinforcements component and here the situation from the previous case repeats, the values are higher than in 15˚ of rotation but are still not near the expected values. At this rotation angle with similar conditions the average max. principal stress value obtained by David is 11.7MPa which is considerably higher than the highest value of 3.3MPa obtained in Figure 49.

Once again, the other components were checked, and again the values on the other major ligaments did not suffer any major change from 15˚ to 30˚.

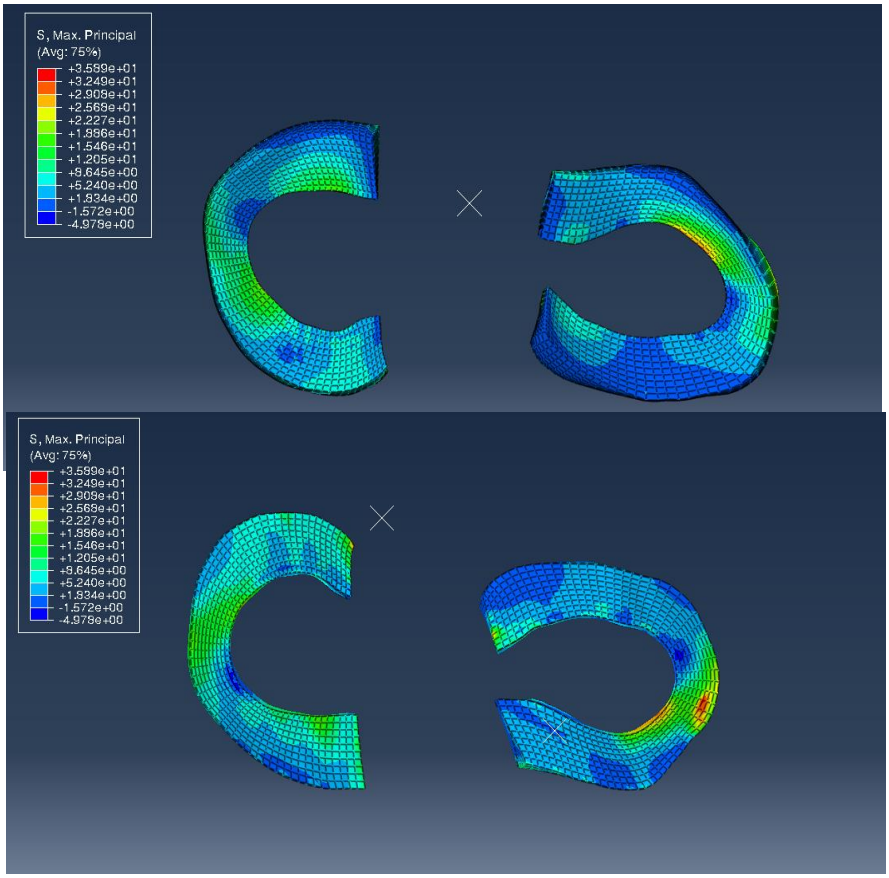

Figure 6.16 – Case 3, Max. Principal Stress on the Medial and Lateral Meniscus, superior and inferior view.

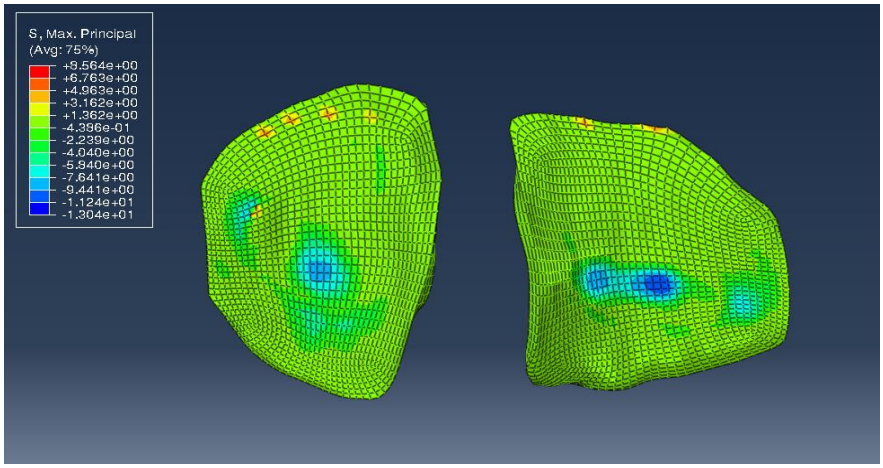

Figure 6.17 – Case 3, Max. Principal Stress on the Left and Right Tibial Cartilage

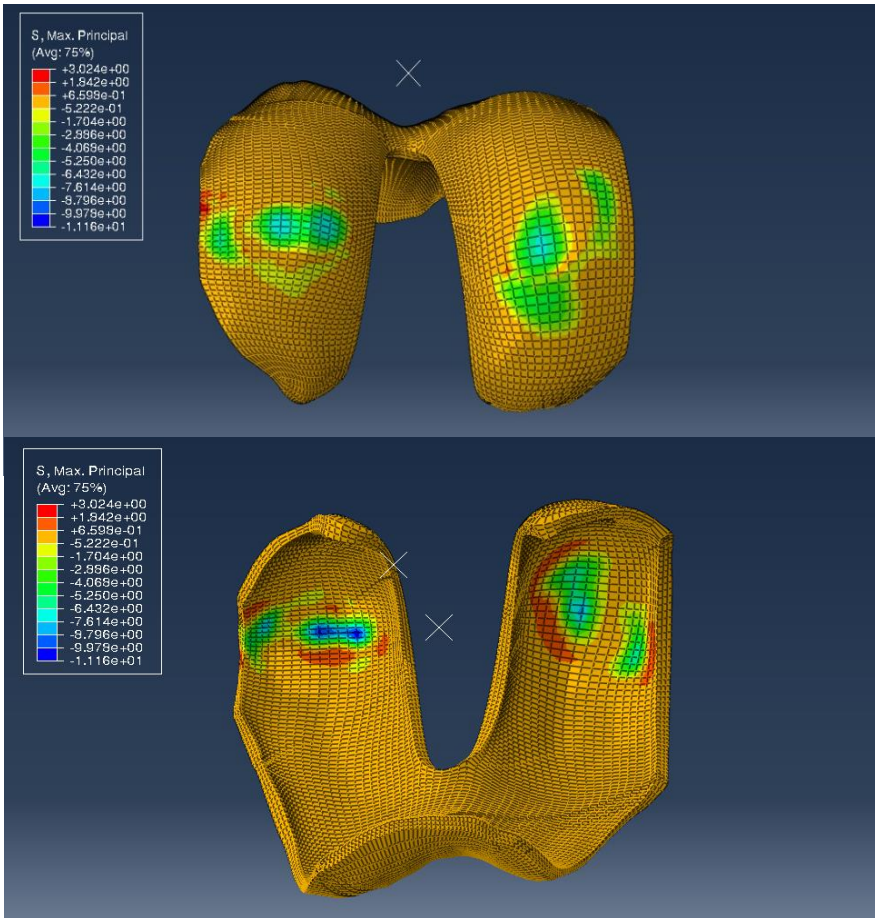

Figure 6.18 – Case 3, Max. Principal Stress on the Femoral Cartilage

Figure 50 to 52 show the max. principal stress results for the Menisci and the Cartilaginous components.

Figure 50 looks at the menisci, and from it, it is seen that the maximum stress values reach the 36.9 MPa, an interesting point here is that this maximum value is lower than when at 15˚ of rotation but the average stress distribution is higher, at around 15 MPa. The higher values, in this flexion angle, are now located in the Lateral Meniscus though most of the stress still is applied in the Medial Meniscus.

Examining now figure 51 and 52, the Femoral and Tibial cartilage possess, once again, high max principal stress values, this time the representation of the stress being prominent on both of the areas that are in direct contact with the menisci, showing the increase in stress distribution throughout the entire area of each of the menisci.

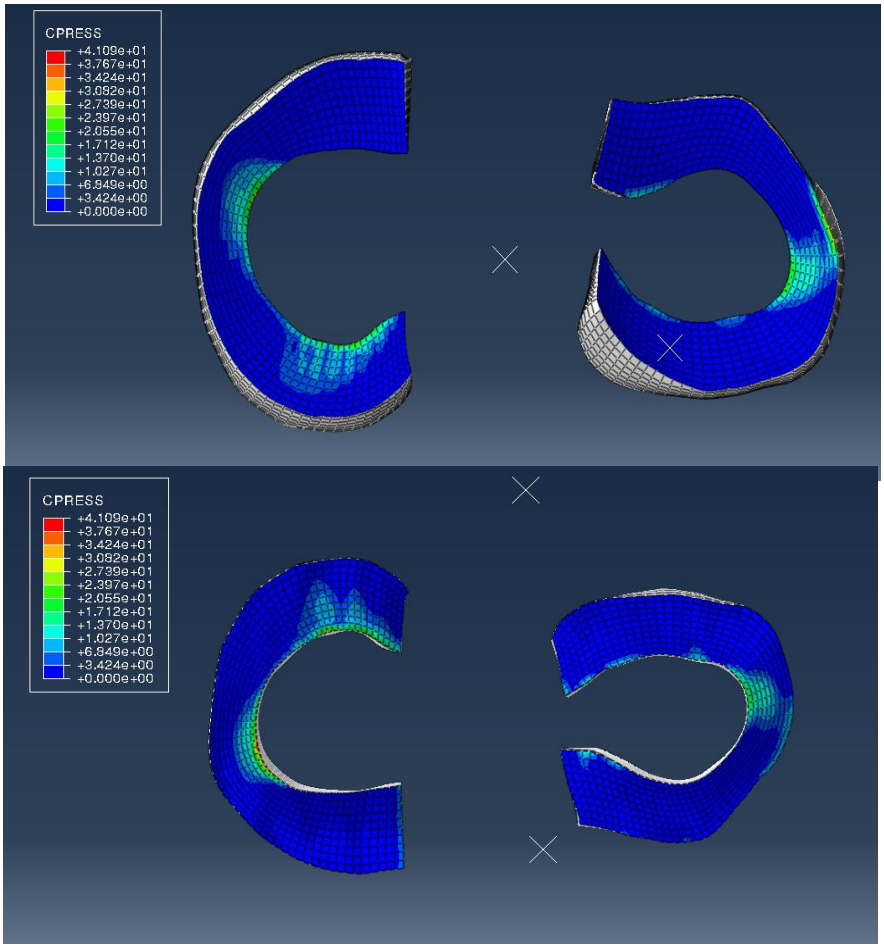

Figure 6.19 – Case 3, Contact Pressure on the Lateral and Mediual Meniscus, superior and inferior view

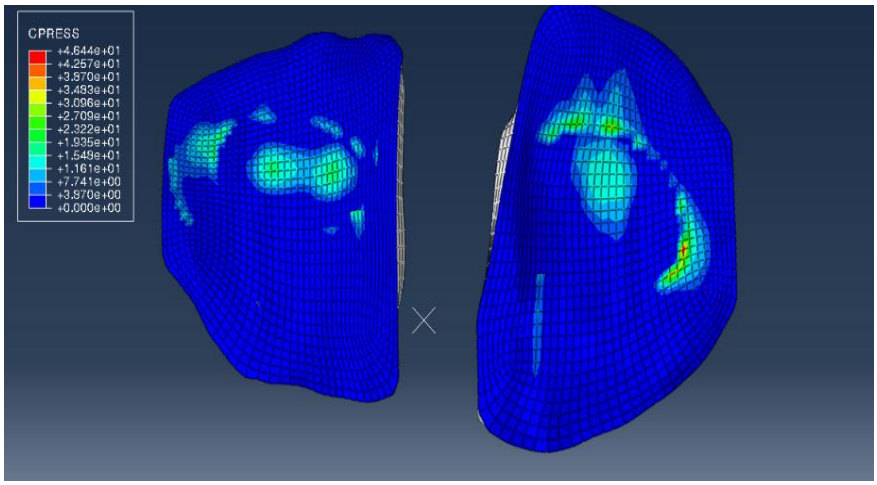

Figure 6.20 – Case 3, Contact Pressure on the Left and Right Tibial Cartilage

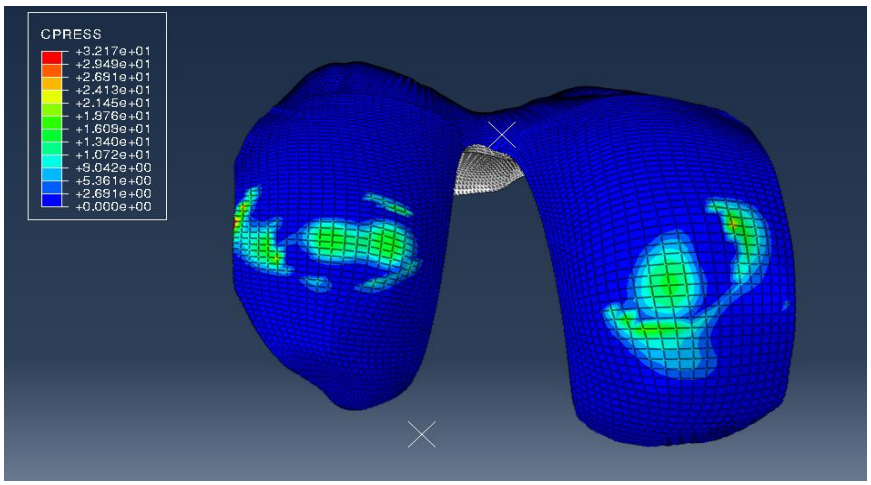

Figure 6.21 – Case 3, Contact Pressure on the Femoral Cartilage

Figure 53 to 55 show the results for the contact pressure on the menisci and the cartilaginous component of the model.

Generally, the same conclusions can be taken as in the previous case, the values for contact pressure presented are higher than what is normal for these components under the same conditions. One difference is that, with both meniscus under higher average stress values the average contact pressure will also increase, this is visually evidenced by the increase in the areas with higher contact pressure values in both figure 54 and 55. One interesting aspect is that the values for contact pressure themselves have not significantly changed from 15° to 30° of rotation the only aspect that has changes is the distribution of these values with the case of 30° of rotation showing more areas with higher values than the case of 15° of rotation.

As for the Tibial and Femoral Cartilage, in figure 54 and 55, the notable difference from the previous case is, as mentioned above, that areas that are affected with high contact pressure on both sides are more pronounced almost giving the outline of the menisci shape.

Chapter 7

Conclusion and Future work

In this work the efficacy of synthetic reinforcement grafts in keeping the biomechanical integrity of the knee joint was studied by applying a posterior femoral force on a Finite Element model of the knee joint.

7.1 - Conclusion

In order to achieve the main objective of this study, many hurdles had to be overcome.

The main issue encountered was the lack of literature on this theme. Unfortunately, there aren't many papers written on the use of Finite Element computerized simulation to study the biomechanical characteristics and performance of synthetic reinforcement grafts in the human knee joint. This considerably limited the initial data and information that was possible to access as well as comparable data.

This issue leaded to another, which was obtaining the material mechanical properties for the various components of the model.

As mentioned previously the knee joint is an incredibly complex structure and if a model is to be created that simulates this structure accurate values and methodologies to characterize each of its components is needed.

Fortunately, the book "FEM Analysis of the Human Knee Joint: A Review" [24] was incredibly useful in gathering data on most of the model's components, but even with this, various tests had to be performed in order to determine which results were the more realistic.

As for the reinforcement, since the type of tests that were executed here have not been done previously, finding the HGO variables to use on this model proved to be quite the challenge.

Like mentioned previously, obtaining these values was only possible through the Online Materials Information Resource (MatWeb) [83], in which there was an overview of the material properties of PET polyester, and the use of the simplified HGO equations.

Because of what is stated above it is important to note that since these values were taken from a general PET polyester material data source, the results may have some inherent errors because the values used here, even though they make a good degree of sense for the situation they are used in, may not be exactly equal to a real synthetic reinforcement graft.

With all the hurdles overcome, the tests were performed, and the results obtained. Through these it was possible to conclude that the model is in a working state capable, at the very least, of providing qualitative data.

The simulations performed show that the synthetic reinforcement, with the material properties given here, does not provide enough biomechanical stability to the knee structure as evidenced by the low values of max principal stress shown in both rotation cases. These in turn caused an increase in the general workload of the menisci and cartilaginous components, showing higher than normal max principal stress and contact pressure values and distribution.

If these values were to happen on a real patient the possibility of further damage being done to the knee joint, more specifically to the overworked components, would be very high.

Unfortunately, some tests were not possible to perform with the current model mainly because of time constraints. One test, that was planned to be performed, was the simulation of a reinforced ACL with missing superficial tissue, this would serve as a simulation of a tear in the ligament, the results obtained from this test would serve as another comparison basis for the model's efficacy.

To conclude, as mentioned throughout this work, the FE model developed here has some limitations and intricacies associated with it, but based on the overall results produced it can be affirmed that with more work it can be used to further study the biomechanics of a graft reinforced knee.

7.2 - Future Work

For future work, the model has several points in which it can be improved upon.

The more pressing one is the material property values for the reinforcement, as mentioned previously, for the tests performed here the values used were obtained through research of the PET material itself and its properties used as the variables in the mathematical equations related to HGO.

Since these values were solely from the recorded properties of PET polyester, an inherent error may exist since, looking in respect to LARS, these reinforcements are composed by PET polyester fibres specifically developed for ACL graft reinforcement. Therefore, it would be beneficial to, if possible, contact one of the companies that deals in the production of these reinforcement grafts in order to obtain the accurate values for its material properties.

A change that can be made is the use of the HGO method itself to characterize the behaviour of the ligaments, this method makes it, so these structures are incompressible which does not correspond to reality. Nolan et al. [101] released a study in which it he demonstrated the flaws of the HGO method when used to describe anisotropic hyperelastic structures, and gives an alternative method that uses a modified anisotropic model that reportedly is capable of more accurately represent the anisotropic response to hydrostatic tensile loading for these structures. This new method, if implemented on this model, may improve the results obtained by bringing more realism to the behaviour of the ligaments.

It would also be beneficial to find a way in which pre-stresses could be applied to the model's ligaments and reinforcement, as mentioned previously this would add a layer of realism to the model.

As for the simulations it would be interesting to simulate other types of movements in which the ACL still plays a role in order obtain even more detailed kinematic results, or simp-

ly improve the existing flexion movement until a full motion of walking or running can be performed.

Bibliographic References

[1] M. Adouni, A. Shirazi-Adl, R. Shirazi, "Computational biodynamics of human knee joint in gait: from muscle forces to cartilage stresses", *Journal of Biomechanics*, Vol. 45, Issue 12, 2012, pp. 2149-2156

[2] S. L. Woo, et al., "Biomechanics of knee ligaments", *American Journal of Sports Medicine*, Vol. 27, Issue 4, 1999, pp. 533-543.

[3] S. L. Woo, et al., "Biomechanics of knee ligaments: injury, healing, and repair", *Journal of Biomechanics*, Vol. 39, Issue 1, 2006, pp. 1-20.

[4] M. Darrow, "The KNEE Sourcebook", McGraw-Hill, 2001, 1st edition. pp. 288.

[5] S. L. Woo, et al., "Tensile properties of the human femur-anterior cruciate ligament-tibia complex. The effects of specimen age and orientation", *American Journal of Sports Medicine*, Vol. 19, Issue 3, 1991, pp. 217-225.

[6] A. D. Orsi, et al., "The effects of knee joint kinematics on anterior cruciate ligament injury and articular cartilage damage", *Computer Methods Biomechanics Biomedical Engineering*, Vol. 19, Issue 5, 2016, pp. 493-506.

[7] S. G. McLean, K.F. Mallett, and E.M. Arruda, "Deconstructing the anterior cruciate ligament: what we know and do not know about function, material properties, and injury mechanics", *Journal of Biomechanical Engineering*, Vol. 137, Issue 2, 2015, pp. 020906.

[8] F. H. Netter, M. J. Timmons, R. B. Tallitsch, "*Human Anatomy*", 7th ed, Pearson, 2011.

[9] E. Alentorn-Geli, et al., "Prevention of anterior cruciate ligament injuries in sports. Part I: systematic review of risk factors in male athletes", *Knee Surg Sports Traumatol Arthrosc*, Vol. 22, Issue 1, 2014, pp. 3-15.

[10] M. Loes, L. Dahlstedt, R. Thomee, "A 7-year study on risks and costs of knee injuries in male and female youth participants in 12 sports", *Scand J Med Sci Sports*, Vol 10, Issue 2, 2000, pp. 90-97.

[11] K. Oberhofer, et al., "The influence of muscle-tendon forces on ACL loading during jump landing: a systematic review", *Muscles, Ligaments and Tendons J*ournal, Vol. 7, Issue 1, 2017, pp. 125-135.

[12] G. Limbert, M. Taylor, and J. Middleton, "Three-dimensional finite element modelling of the human ACL: simulation of passive knee flexion with a stressed and stress-free ACL", *Journal of Biomechanics*, Vol. 37, Issue 11, 2004, pp. 1723-1731.

[13] Z. Machotka, et al., "Anterior cruciate ligament repair with LARS (ligament advanced reinforcement system): a systematic review", *Sports Med Arthrosc Rehabil Ther Technol*, Vol. 2, Issue 29, 2010, pp. 29.

[14] A. Kiapour, et al., "Finite element model of the knee for investigation of injury mechanisms: development and validation", *Journal of Biomechanical Engineering*, Vol. 136, Issue 1, 2014, pp. 011002.

[15] G. DeMorat, et al., "Aggressive quadriceps loading can induce noncontact anterior cruciate ligament injury", *American Journal of Sports Medicine*, Vol. 32, Issue 2, 2004, pp. 477-483.

[16] E. G. Meyer, R.C. Haut, "Anterior cruciate ligament injury induced by internal tibial torsion or tibiofemoral compression", *J Biomech*, Vol. 41, Issue 16, 2008, pp. 3377-3383.

[17] D. B. Lipps, et al., "Morphologic characteristics help explain the gender difference in peak anterior cruciate ligament strain during a simulated pivot landing", *American Journal of Sports Medicine*, Vol. 40, Issue 1, 2012, pp. 32-40.

[18] M. Majewski, H. Susanne, S. Klaus, "Epidemiology of athletic knee injuries: A 10-year study", *The Knee*, Vol. 13, Issue 3, 2006, pp. 184-188.

[19] K. R. Ford, G.D. Myer, and T.E. Hewett, "Valgus knee motion during landing in high school female and male basketball players", *Med Sci Sports Exerc*, Vol. 35, Issue 10, 2003, pp. 1745-1750.

[20] H. Koga, et al., "Mechanisms for noncontact anterior cruciate ligament injuries: knee joint kinematics in 10 injury situations from female team handball and basketball", *American Journal of Sports Medicine*, Vol. 38, Issue 11, 2010, pp. 2218-2225.

[21] E. Pena, et al., "A three-dimensional finite element analysis of the combined behavior of ligaments and menisci in the healthy human knee joint", *Journal of Biomechanics*, Vol. 39, Issue 9, 2006, pp. 1686-1701.

[22] F. Xie, et al., "A study on construction three-dimensional nonlinear finite element model and stress distribution analysis of anterior cruciate ligament", *Journal of Biomechanical Engineering*, Vol. 131, Issue 12, 2009, pp. 121007.

[23] Y. Song, et al., "A three-dimensional finite element model of the human anterior cruciate ligament: a computational analysis with experimental validation", *Journal of Biomechanics*, Vol. 37, Issue3, 2004, pp. 383-390.

[24] Z. Trad, A. Barkaooui, M. Chafra, J. Tavares, "*FEM Analysis of the Human Knee Joint: A Review*", Springer International Publishing, 1st ed, 2018.

[25] S. Hirokawa, R. Tsuruno, "Three-dimensional deformation and stress distribution in an analytical/computational model of the anterior cruciate ligament", *Journal of Biomechanics*, 2000. **33**(9): p. 1069-77.

[26] K. E. Moglo, A. Shirazi-Adl, "Biomechanics of passive knee joint in drawer: load transmission in intact and ACL-deficient joints", The Knee, Vol. 10, Issue 3, 2003, pp. 265-76.

[27] H. Strasser, "*Lehrbuch der Muskel und Gelenkmechanik*". *Z Anat Entwickl*, Vol. 83, 1917, pp. 752–770

[28] S. Burguess, "Critical characteristics and the irreducible knee joint", *Ans Genesis*, Vol. 13, 1999, pp. 112-117.

[29] G. Steven, et all., "The influence of four-bar linkage knees on prosthetic swing-phase floor clearance", *Journal of Prosthetics and Orthotics*, Vol. 8, Issue 2, 1996, pp. 34-40.

[30] R. Huiskes, L. Blankevoort, *"Anatomy and Biomechanics of the Anterior Cruciate Ligament: A Three-Dimensional Problem"*, Springer, Berlin, Heidelberg, 1990.

[31] C. Wan, Z. Hao, S. Wen, "The effect of the variation in ACL constitutive model on joint kinematics and biomechanics under different loads: a finite element study", *Journal of Biomechanical Engineering*, Vol. 135, Issue 4, 2013, pp. 041002.

[32] A. Menschik, "Mechanics of the knee-joint, part 1", *Z Orthop Ihre Grenzgeb* ,Vol. 112, Issue 3, 1974, pp. 481-495.

[33] F. K. Fuss, "Anatomy of the cruciate ligaments and their function in extension and flexion of the human knee joint", *Am J Anat*, Vol. 184, Issue 2, 1989, pp. 165-176.

[34] H. S. Park, et al., "A knee-specific finite element analysis of the human anterior cruciate ligament impingement against the femoral intercondylar notch", *J Biomech*, Vol. 43, Issue 10, 2010, pp. 2039-2042.

[35] B. J. Ellis, et al., "Medial collateral ligament insertion site and contact forces in the ACL-deficient knee", *J Orthop Res*, Vol. 24, Issue 4, 2006, pp. 800-810.

[36] Y. Dhaher, T.H. Kwon, M. Barry, "The effect of connective tissue material uncertainties on knee joint mechanics under isolated loading conditions", *J Biomech*, Vol. 43, Issue 16, 2010, pp. 3118-3125.

[37] E. Pena, et al., "A finite element simulation of the effect of graft stiffness and graft tensioning in ACL reconstruction", *Clin Biomech (Bristol, Avon)*, Vol. 20, Issue 6, 2005, pp. 636-644.

[38] T. L. Donahue, et al., "A finite element model of the human knee joint for the study of tibio-femoral contact", *J Biomech Eng*, Vol. 124, Issue 3, 2002, pp. 273-280.

[39] Yuhua Song, Richard E. Debski, Volker Musahl, Maribeth Thomas, Savio L.-Y. Woo, "A three-dimensional finite element model of the human anterior cruciate ligament: a computational analysis with experimental validation", Journal of Biomechanics, Vol. 37, Issue 3, 2004, pp 383-390.

[40] J. M. Penrose, et al., "Development of an accurate three-dimensional finite element knee model", *Comput Methods Biomech Biomed Engin*, Vol. 5, Issue 4, 2002, pp. 291-300.

[41] J. P. Halloran, A.J. Petrella, P.J. Rullkoetter, "Explicit finite element modeling of total knee replacement mechanics", *J Biomech*, Vol. 38, Issue 2, 2005, pp. 323-331.

[42] G. Limbert, J. Middleton, M. Taylor, "Finite element analysis of the human ACL subjected to passive anterior tibial loads", *Comput Methods Biomech Biomed Engin*, Vol. 7, Issue 1, 2004, pp. 1-8.

[43] W. Andrew, February 04, 2020, "*Human skeleton ANATOMY*", Enciclopaedia Britannica [Online], Available: https://www.britannica.com/science/human-skeleton/Axial-and-visceral-skeleton#info-article-history, Quoted in 21/June/2020.

[44] I. Peat, "*Fundamentals of Anatomy and Physiology: For Nursing and Healthcare Students*", pp. 656, John Wiley and Sons Ltd, 2016.

[45] J. Fernando, et all., "Estrutura e Dinâmica do Tecido Ósseo", Clínica Universitária de Ortopedia, 2012.

[46] Types of Synovial Joints, Lumen Biology for Majors, Available: https://courses.lumenlearning.com/wm-biology2/chapter/types-of-synovial-joints/, Quoted in 21/June/2020.

[47] N. M. Willems, et al., "The microstructural and biomechanical development of the condylar bone: a review", *Eur J Orthod*, Vol. 36, Issue 4, 2014, pp. 479-485.

[48] Natural Height Growth, February 2014, Available from: http://www.naturalheightgrowth.com/2014/02/01/update-11-decalcification-bone-layer-february-1-2014/, Quoted in 21/June/2020

[49] Classification of bones by shape, February 1st, 2014, Available from: https://slideplayer.com/slide/8238756/, Quoted in 21/June/2020.

[50] T. Khuvasanont, "Age-Related Ankle Strength Degradation and Effects on Slip-Induced Falls", Virginia Polytechnic Institute and State University, Thesis for Master of Science in Industrial and Systems Engineering, 2002.

[51] F. Shereen, M. Elmessiry, "Study of the Effect of Cyclic Stress on the Mechanical Properties of Braided Anterior Cruciate Ligament (ACL)", Journal of Textile Science and Engineering, Vol. 6, 2016.

[52] Basic Sciences, Decembre 26, 2016, Available from: https://musculoskeletalkey.com/basic-sciences/, Quoted in 21/June/2020

[53] G. J. Tortora, *"Introduction to the Human Body: The Essentials of Anatomy and Physiology"*, 8th edition 2009: John Wiley & Sons. 704.

[54] A. J. Fox, et al., "The human meniscus: a review of anatomy, function, injury, and advances in treatment", *Clin Anat*, Vol. 28, Issue 2, 2015, pp. 269-287.

[55] S. Hall, "*Basic Biomechanics*", 6 ed, 2012: McGraw-Hill Education.

[56] S. Gupta, V. Ponemone, M. Suthar, "Emerging potential of cell based therapies for articular cartilage repair and regeneration", *Advances in Tissue Engineering and Regenerative Medicine*, 2017.

[57] K. Andrews, et al., "Review: Medial collateral ligament injuries", *J Orthop*, Vol. 14,Issue 4, 2017, po. 550-554.

[58] J. Oliver, *TeachMe Anatomy*, 11/July/2019, Available from: https://teachmeanatomy.info/lower-limb/joints/knee-joint/, Quoted at 26/Jan/2020.

[59] S. Pache, et al., "Posterior Cruciate Ligament: Current Concepts Review", *Arch Bone Jt Surg*, Vol. 6, Issue 1, 2018, pp. 8-18.

[60] R. Balius, C. Pedret, Avances Ecográficos en Patología Tendinosa, 2017, Available from: https://docplayer.es/83460775-Molecula-colageno-tipo-1.html, Quoted at 26/Jan/2020.

[61]M. A. Haddad, J.M. Budich, B.J. Eckenrode, "Conservative Management of an Isolated Grade Iii Lateral Collateral Ligament Injury in an Adolescent Multi-Sport Athlete: A Case Report", *Int J Sports Phys Ther*, Vol. 11, Issue 4, 2016, pp. 596-606.

[62] U. M. Kujala, et al., "Acute injuries in soccer, ice hockey, volleyball, basketball, judo, and karate: analysis of national registry data", *Journal of Biomechanics*, Vol. 311, Issue 7018, 1995, pp. 1465-1468.

[63] S. M. Gianotti, et al., "Incidence of anterior cruciate ligament injury and other knee ligament injuries: a national population-based study", *J Sci Med Sport*, Vol. 12, Issue 6, 2009, pp. 622-627.

[64] S. B. Cohen, et al., "Factors affecting patient selection of graft type in anterior cruciate ligament reconstruction", *Arthroscopy*, Vol. 25, Issue 9, 2009, pp. 1006-1010.

[65] L. M. Tibor, et al., "Clinical outcomes after anterior cruciate ligament reconstruction: a meta-analysis of autograft versus allograft tissue", *Sports Health*, Vol. 2, Issue 1, 2010. pp. 56-72.

[66] R. Mascarenhas, P.B. MacDonald, "Anterior cruciate ligament reconstruction: a look at prosthetics--past, present and possible future", *Mcgill J Med*, Vol. 11, Issue 1, 2008, pp. 29-37.

[67] K. Trieb, et al., "In vivo and in vitro cellular ingrowth into a new generation of artificial ligaments", *Eur Surg Res*, Vol. 36, Issue 3, 2004, pp. 148-151.

[68] *Everything you Need to Know About The World's Most Useful Plastic (PET and Polyester)*, 2016 , Available: https://www.creativemechanisms.com/blog/everything-about-polyethylene-terephthalate-pet-polyester, Quoted at 21/June/2020

[69] *An Introduction to PET (polyethylene terephthalate)*, PETRA, Available: http://www.petresin.org/news_introtoPET.asp, Quoted at 21/June/2020

[70] LARS, Corin Australia, Available from: https://www.coringroup.com/au/solutions/lars/, Quoted at 26/Jan/2020

[71] M. Zuzana, et all., "Ligament Advanced Reinforcement system anterior cruciate ligament reconstruction", *Sports Medicine Arth Reh Ther and Tech*, Vol. 3, 1995, pp. 187-205.

[72] L. M. Batty, et al., "Synthetic devices for reconstructive surgery of the cruciate ligaments: a systematic review", *Arthroscopy*, Vol. 31, Issue 5, 2015, pp. 957-968.

[73] K. Gao, et al., "Anterior cruciate ligament reconstruction with LARS artificial ligament: a multicenter study with 3- to 5-year follow-up" *Arthroscopy*, Vol. 26, Issue 4, 2010, pp. 515-523.

[74] C. M. Glezos, et al., "Disabling synovitis associated with LARS artificial ligament use in anterior cruciate ligament reconstruction: a case report", *Am J Sports Med*, Vol. 40, Issue 5, 2012, pp. 1167-1171.

[75] H. Li, et al., "Biologic failure of a ligament advanced reinforcement system artificial ligament in anterior cruciate ligament reconstruction: a report of serious knee synovitis", *Arthroscopy*, Vol. 28, Issue 4, 2012, pp. 583-586.

[76] M. F. Nordin, et all., "*Basic biomechanics of the musculoskeletal system*", pp. 323, Lea & Febiger, ed. 4, 12/Jan/2012.

[77] A. Hollister, et all., "The Axes of Rotation of the Knee", *Clin Orthop Telat Res*, Vol. 290, 1993, pp. 259-268.

[78] A. Azevedo, "*MÉTODO DOS ELEMENTOS FINITOS*", Faculdade de Engenharia da Universidade do Porto, 2003.

[79] T. English, "What Is Finite Element Analysis and How Does It Work?", 2019, Available: https://interestingengineering.com/what-is-finite-element-analysis-and-how-does-it-work, Quoted at 21/June/2020

[80] D. Carvalho, "Estudo Biomecânico dos Meniscos na Articulação do Joelho Humano", Faculdade de Engenharia da Universiade do Porto, Dissertação de Mestrado, 2015.

[81] Scott Sibole, Craig Bennets, Bhusha Borotikar, Steve Maas, Ahmet Erdemir, "Open Knee: A 3D Finite Element Representation of the Knee Joint", American Siciety of Biomechanics Annual Conference, 2008; 1058-1059.

[82] Systemes, D., *Abaqus 6.10 Analysis Guide*, 2010.

[83] Data, M.-M.P., *Overview of materials for Polycarbonate/PET Polyester Blend*.

[84] Eihab Muhammed Abdel-Rahman, Mohamed Samir Hefzy., "Threedimensional dynamic behaviour of the human knee joint under impact loading", Medical Engineering & Physics, Vol. 20, Issue 4, 1998, pp 276–290.

[85] B. J. Ellis, et al., "Methodology and sensitivity studies for finite element modeling of the inferior glenohumeral ligament complex", *Journal of Biomechanics*, Vol. 40, Issue 3, 2007, pp. 603–612

[86] S. M. Moore, et al., "The glenohumeral capsule should be evaluated as a sheet of fibrous tissue: a validated finite element model", *Annals of Biomedical Engineering*, Vol. 38, Issue 1, 2010, pp. 66–76

[87] P. Łuczkiewicz, K. Daszkiewicz, J. Chróscielewski, W. Witkowski, P. J. Winklewski, "The influence of articular cartilage thickness reduction on meniscus biomechanics", PLoS ONE, Decembre 9, 2016., 11(12).

[88] P. Beillas, et al., "A new method to investigate in vivo knee behavior using a finite element model of the lower limb", *Journal of Biomechanics*, Vol. 37, Issue 7, 2004, pp. 1019–1030.

[89] D. Anderson, T. Brown, E. Radin, "The influence of basal cartilage calcification on dynamic juxtaarticular stress transmission", Clinical Orthopaedics and Related Research, 1993, pp 286–307

[90] H. Wei, et al., "The influence of mechanical properties of subchondral plate, femoral head and neck on dynamic stress distribution of the articular cartilage", *Medical Engineering & Physics*, Vol. 27, Issue 4, 2005, pp. 295–304

[91] J. C. Gardiner, J. A. Weiss, "Subject-specific finite element analysis of the human medial collateral ligament during valgus knee loading", *Journal of Orthopaedic Research*, Vol. 21, Issue 6, 2003, pp. 1098– 1106.

[92] E. Peña, B. Calvo, M. A. Martínez, M. Doblaré, "A three-dimensional finite element analysis of the combined behavior of ligaments and menisci in the healthy human knee joint", *Journal of Biomechanics*, Vol. 39, Issue 9, 2006, pp 1686-1701.

[93] T. C. Gasser, R.W. Ogden, G.A. Holzapfel, "Hyperelastic modelling of arterial layers with distributed collagen fibre orientations", *J R Soc Interface*, Vol. 3, Issue 6, 2006. pp. 15-35.

[94] G. A. Holzapfel, T. C. Gasser, R. Ogden, "A New Constitutive Framework for Arterial Wall Mechanics and a Comparative Study of Material Models," Journal of elasticity and the physical science of solids, Vol. 61, Issue 1, 2000, pp. 1–48.

[95] G. Holzapfel, T. Gasser, "A viscoelastic model for fiber-reinforced composites at finite strains: Continuum basis, computational aspects and applications", Computer Methods in Applied Mechanics and Engineering, Vol. 190, 2001, pp. 4379–4403.

[96] R. W. Westermann, B.R. Wolf, J.M. Elkins, "Effect of ACL reconstruction graft size on simulated Lachman testing: a finite element analysis", *Iowa Orthop J*, Vol. 33, 2013, pp. 70-77.

[97] Systeme, D., *Abaqus 6.10 Theory Manual*. 2010.

[98] D. Fernandes, "Finite Element Analysis of the ACL-deficient Knee", Universidade Técnica de Lisboa, Dissertação de Mestrado, 2014

[99] D. John, D. Pinisetty, N. Gupta, "Image Based Model Development and Analysis of the Human Knee Joint", Andreaus U., Iacoviello D. (eds) Biomedical Imaging and Computational Modeling in Biomechanics, Lecture Notes in Computational Vision and Biomechanics, Dordrecht, Springer, 2013, vol 4.

[100] D. P. John, N. Gupta, "Image Based Model Development and Analysis of the Human Knee Joint", *B.I.a.C.M.i. Biomechanics*, 2013, pp. 55-79.

[101] D. R. Nolan, et al., "A robust anisotropic hyperelastic formulation for the modelling of soft tissue", *J Mech Behav Biomed Mater*, Vol. 39, 2014, pp. 48-60.

Appendix

```
**********************************************************************************************************************
**********************************************************************************************************************
**                                        Knee Model
**********************************************************************************************************************
**********************************************************************************************************************
*include,input=nodes_com_acl_total.inp
*include,input=estruturas.inp
*include,input=surfaces_total_new_menisco.inp
*include,input=materials_hgo_paper_kzero.inp
*include,input=ties.inp
*include,input=contactos.inp
*include,input=ABQsprings8_barra_newmenisco.inp
*include,input=menisco_lig.inp
*include,input=lig_knee.inp
**
**
**
**********************************************************************************************************************
**                              Step 1 - Apply rotation   flexing X graus
**********************************************************************************************************************
**
** begin step, nonlinear geometry
*step,nlgeom,inc=10000
**
**static load step, initial time increment (0.05), step time period (1.0), max time incre-
ment(1e-6)
*static
0.05, 1.0, 1e-6
**
**reset all values to default
*Controls, reset
**set analysis as discontinuous
*Controls, analysis=discontinuous
**
**
*CONTACT CONTROLS, STABILIZE=0.5
**
**set velocity history
*boundary, type=velocity
**
** node 20584 (on the Tibia), constrained on all degrees of freedom
20584,1,6,0.0
**
** node 2749 (on the Femur), constrained so that no rotation happens on the X and Y axis
2749,4,5,0.0
```

```
** node 2749 (on the Femur), rotates on the Z axis (X=0.52 radians = 30 degrees / X=0.26 radians = 15 degrees / X=0.0 radians = 0 degrees)
2749,6,6,X
**
**
**
*end step
**********************************************************************************************************************
**                          Step 2 - Apply Force
**********************************************************************************************************************
*step,nlgeom,inc=10000
**
**static load step, initial time increment (0.05), step time period (1.0), max time increment(1e-6)
*static
0.05, 1.0, 1e-10
**
**reset all values to default
*Controls, reset
**set analysis as discontinuous
*Controls, analysis=discontinuous
**
**set velocity history
*boundary, type=velocity
**
** node 20584 (on the Tibia), constrained on all degrees of freedom
20584,1,6,0.0
**
**
**node 2749 (on the Femur), constrained so that no rotation happens on the Z axis
2749,6,6,0.0
**
**
**A Force is applied on the node 2749 (on the Femur) with X Newtons
*cload
2749, 6, X
**
**
*end step
******************************************************
**********************************************************************************************************************
**********************
```